Alexandrium fundyense cysts in the Gulf of Maine: long-term time series of abundance and distribution, and linkages to past and future blooms

Donald M. Anderson[a,*], **Bruce A. Keafer**[a], **Judith L. Kleindinst**[a], **Dennis J. McGillicuddy Jr.**[a], **Jennifer L. Martin**[b], **Kerry Norton**[a], **Cynthia H. Pilskaln**[c], **Juliette L. Smith**[a], **Christopher R. Sherwood**[d], and **Bradford Butman**[d]

[a]Woods Hole Oceanographic Institution, Woods Hole, MA 02543 USA

[b]Fisheries and Oceans Canada, Biological Station, St. Andrews, NB E5B 2L9, Canada

[c]School for Marine Science and Technology, Univ. of Massachusetts Dartmouth, New Bedford, MA 02744 USA

[d]US Geological Survey, Woods Hole, MA 02543 USA

Abstract

Here we document *Alexandrium fundyense* cyst abundance and distribution patterns over nine years (1997 and 2004-2011) in the coastal waters of the Gulf of Maine (GOM) and identify linkages between those patterns and several metrics of the severity or magnitude of blooms occurring before and after each autumn cyst survey. We also explore the relative utility of two measures of cyst abundance and demonstrate that GOM cyst counts can be normalized to sediment volume, revealing meaningful patterns equivalent to those determined with dry weight normalization.

Cyst concentrations were highly variable spatially. Two distinct seedbeds (defined here as accumulation zones with > 300 cysts cm^{-3}) are evident, one in the Bay of Fundy (BOF) and one in mid-coast Maine. Overall, seedbed locations remained relatively constant through time, but their area varied 3-4 fold, and total cyst abundance more than 10 fold among years. A major expansion of the mid-coast Maine seedbed occurred in 2009 following an unusually intense *A. fundyense* bloom with visible red-water conditions, but that feature disappeared by late 2010. The regional system thus has only two seedbeds with the bathymetry, sediment characteristics, currents, biology, and environmental conditions necessary to persist for decades or longer. Strong positive correlations were confirmed between the abundance of cysts in both the 0-1 and the 0-3 cm layers of sediments in autumn and geographic measures of the extent of the bloom that occurred the next year (i.e., *cysts → blooms*), such as the length of coastline closed due to shellfish toxicity or the southernmost latitude of shellfish closures. In general, these metrics of bloom geographic extent

---

*Corresponding author. Tel: +1 508 289 2351; Fax: +1 508 457 2027; danderson@whoi.edu.

did not correlate with the number of cysts in sediments following the blooms (*blooms → cysts*). There are, however, significant positive correlations between 0-3 cm cyst abundances and metrics of the preceding bloom that are indicative of bloom intensity or vegetative cell abundance (e.g., cumulative shellfish toxicity, duration of detectable toxicity in shellfish, and bloom termination date). These data suggest that it may be possible to use cyst abundance to empirically forecast the geographic extent of the forthcoming bloom and, conversely, to use other metrics from bloom and toxicity events to forecast the size of the subsequent cyst population as the inoculum for the next year's bloom. This is an important step towards understanding the excystment/encystment cycle in *A. fundyense* bloom dynamics while also augmenting our predictive capability for this HAB-forming species in the GOM.

Keywords

1 Introduction

Many harmful algal bloom (HAB) species produce dormant cysts or resting spores during their life histories. The resulting alternation between a dormant, benthic stage and a motile, vegetative existence is critically important in many aspects of bloom dynamics. Cyst germination provides an inoculum for blooms, and cyst formation can remove substantial numbers of cells from blooms as they terminate. Cysts also have other important ecological roles such as species dispersal, survival through adverse conditions, and genetic recombination when sexuality is involved in their formation (Wall, 1971).

Dinoflagellate resting cysts accumulate in bottom sediments (e.g., Anderson et al., 1982) or near-bottom nepheloid layers (Kirn et al., 2005; Pilskaln et al., this issue-b); the amount of time spent in dormant or quiescent states (Pfiester and Anderson, 1987) is determined by both internal and external factors. Internal regulation includes a mandatory maturation period after cysts are formed that can prevent germination for days to months depending on the species (e.g., Anderson, 1980; Bravo and Anderson, 1994) and, for some species, an endogenous annual clock as observed in *Alexandrium fundyense* (Anderson and Keafer, 1987; Matrai et al., 2005). External regulation includes temperatures that inhibit germination above and below a "window" or permissive range (Dale, 1983; Anderson, 1998), and light, which is required by some species for germination or which speeds up the germination process compared to its rate in darkness (Anderson et al., 1987, 2005c). Most dinoflagellate species have an absolute requirement for oxygen during germination (Anderson et al., 1987; Rengefors and Anderson, 1998; Kremp and Anderson, 2000). Cysts buried deep in the sediment can thus remain quiescent for many years (decades to as long as a century (Ribeiro et al. 2011; Miyazono et al., 2012)), their fate being either eventual death if anoxia persists, or germination should they be transported to oxic conditions in the sediment surface or overlying water via physical processes or bioturbation.

Clearly, the location of cyst accumulations in bottom sediments (termed "seedbeds") can be an important determinant of the location of resulting blooms, and the size of the cyst

populations and the timing and extent of excystment and encystment can directly affect the magnitude of the blooms in some regions (Wall, 1971; Anderson, 1998; McGillicuddy et al., 2011). Surveys of the distribution and abundance of cysts can therefore be very useful in ecological and monitoring studies. Historically, such mapping studies have been used to define the geographic range of a particular HAB species (e.g., Anderson, et al., 1982; Imai et al., 1991), to identify potential seedbeds for bloom initiation (e.g., Tyler et al., 1982) or sites for monitoring (Anderson et al., 1982; Hattenrath et al., 2010), to study the dispersal of an organism from one region to another (e.g., Imai et al., 1991; Anderson et al., 1982), or for use in numerical models of HAB population dynamics (McGillicuddy et al., 2003, 2005; Anderson et al., 2005c; Stock et al. 2005; He et al., 2008).

The concept of a discrete seedbed may not be appropriate in some locations due to the widespread, dispersed distribution of some cysts and the likelihood that germination will therefore occur over a large area. In many areas, however, there is evidence for localized cyst accumulations, both in estuarine systems and in deeper coastal waters. Within the shallow Nauset Marsh System on Cape Cod, for example, surveys revealed three highly localized *A. fundyense* cyst seedbeds at the extreme ends of the complex network of channels and salt ponds that comprise that system (Crespo et al., 2011). Surveys during bloom seasons document the tight link between these seedbeds and the areas of bloom initiation and retention within the system. A similar linkage between cyst seedbeds and localized blooms has been observed in lagoons, harbors, or other such sites in the Mediterranean, such as in Thau Lagoon, France (Genovesi et al., 2009), Cork Harbor, Ireland (Ní Rathaille and Raine, 2011) and Arenys de Mar harbor, Spain (Angeles et al., 2010, 2012).

Examples of cyst seedbeds in deeper coastal waters are less common (e.g., Anderson and Keafer, 1985; Turgeon et al., 1990; Anderson et al., 2005c), presumably due to the expense and difficulty of large-scale mapping. Here we describe the cyst accumulations documented during a nine-year series of large-scale, annual mapping surveys within the Gulf of Maine (GOM) coastal waters (USA and Canada) and examine relationships between those distributions and the magnitude and extent of *A. fundyense* blooms in the years preceding and following each survey. We also present data on the manner in which cysts can be enumerated in surface sediment samples for ecological studies, and on the variability inherent in cyst sampling and counting[1].

These cyst distributions are best understood in the context of GOM hydrography (Fig. 1), of which a dominant feature is the Maine Coastal Current or MCC (Brooks and Townsend, 1989; Lynch et al., 1997; Pettigrew et al., 2005) - a composite of multiple segments and branch points. Conceptual models of *A. fundyense* bloom dynamics within the MCC have been provided by Anderson et al. (2005c) and McGillicuddy et al. (2005). Briefly, key features are two large cyst seedbeds - one in the Bay of Fundy (BOF) and the other offshore of mid-coast Maine (Anderson et al., 2005c). Cysts germinate from the BOF seedbed, causing recurrent blooms within the bay that are self-seeding with respect to future

---

[1]In this study, we have focused on the harmful algal species *Alexandrium tamarense* Group I, which we refer to as *A. fundyense*, the renaming proposed by Lilly et al. (2007).

outbreaks in that area. In effect, the BOF is an incubator for localized populations in that area, but the incubator is leaky (Aretxabaleta et al., 2008, 2009), as cells can be transported into the MCC, where they bloom, particularly at the distal end of the eastern segment of that coastal current, where waters warm and stratify (Townsend et al., 2001). Some cells travel south and west with the MCC, while others deposit cysts in the mid-coast Maine seedbed. In subsequent years, these latter cysts (combined with vegetative cells from populations in the eastern segment of the MCC) initiate blooms that cause toxicity in western portions of the Gulf. Shellfish toxicity along the coast is regulated not only by bloom dynamics but also by coastal current transport, with northeasterly winds accelerating the alongshore and onshore movement of *A. fundyense* populations (Franks and Anderson, 1992a, b; Anderson et al., 2005a).

Given the regional hydrography and bloom dynamics, here we separate the Gulf of Maine (GOM) into three subregions - the western GOM, the eastern GOM, and the Bay of Fundy (WGOM, EGOM, and BOF, respectively; Fig. 1). Although these subregions are linked by the alongshore extension of the MCC, they have unique or individual characteristics and thus are examined separately in the analyses presented here.

2 Methods

2.1 Mapping of cysts in the 0-1 and 1-3 cm sediment layers

All cyst surveys took place in the GOM (Fig. 1) in late September, October or early November, well after new *A. fundyense* cysts had formed and settled from spring and summer blooms, and before any potential germination of mature cysts occurs. The first large-scale survey was conducted November 5-11, 1997 *(R/V Endeavor; EN310)*, with sediment samples collected from 66 stations in offshore and nearshore waters between Portsmouth, New Hampshire and the mouth of the BOF. Cyst counts from this cruise were augmented with another set of counts from 48 stations in Casco Bay and adjacent offshore waters, collected during October 28-31, 1997 on a survey using the R/V *Gulf Challenger*. Subsequently, eight large-scale cyst mapping cruises were completed each fall from 2004 - 2011 on the UNOLS research vessels R/V *Cape Hatteras*, R/V *Oceanus*, or R/V *Endeavor*. These cruises extended the sampling domain to include the BOF and farther offshore than in 1997. The cruises were conducted on October 19-28, 2004 (R/V *Cape Hatteras*; CH1504), September 20-30, 2005 (R/V *Oceanus*; OC416), October 31-November 12, 2006 (R/V *Oceanus*; OC433), October 8-18, 2007 (R/V *Oceanus*; OC440), October 14-24, 2008 (R/V *Endeavor*; EN456), October 15-25, 2009 (R/V *Oceanus*; OC458), Oct 13-23, 2010 (R/V *Endeavor*; EN486), and October 24-November 4 in 2011 (R/V *Oceanus*; OC477).

Samples for these surveys were collected using a hydraulically damped corer (Craib, 1965), which obtains undisturbed sediment samples. At a limited number of stations where the sediment substrate was hard and difficult to obtain with the corer, sediment was collected using a Younge-modifed Van Veen grab sampler. The cores were split into the 0-1 cm and 1-3 cm layers, and a homogenized 5 cm^3 wet sediment sample was collected from each layer for counting, following the methods of Anderson et al. (1982, 2003). During some cruises, another replicate 5 cm^3 volume was saved for determination of cyst concentration by dry weight (see below).

For counting, the sediment was resuspended with filtered (<15μm) seawater, disaggregated with a Branson Sonifier 250D at a constant 40-watt output for 1 minute, and sieved to yield a clean, 20-100 μm size fraction (Anderson et al., 2003). Immediately after sampling at sea, 14 ml of processed sediment were preserved by the addition of 0.75 ml of a 20% formaldehyde solution (1% final) and stored onboard at 2-4°C for at least 24 hours. The sample was then centrifuged (3000 × g) for 10 min and the overlying supernatant removed by aspiration. The pellet was brought up to 10 ml with cold methanol dispensed from a glass solvent container in an ice bath, and stored onboard for at least 48 h at −20° C. At the shore laboratory, the sample was centrifuged and aspirated as before, and 2 ml of primuline stain (2 mg ml^{-1}) was added directly to the pellet. After staining for 1 h, the sample was centrifuged and the supernatant aspirated and brought up to 5 ml in deionized water, or if the particle load was very high, 10 ml was used as a final volume. *Alexandrium fundyense* cysts were counted in 1-ml Sedgewick-Rafter slides according to standard methods for cyst identification and enumeration (Anderson et al., 2003) using primuline to stain the cysts (Yamaguchi et al., 1995) and a Zeiss epi-fluorescence microscope at 100X with a chlorophyll filter set (excitation band pass 450-490 nm, emission long pass 520 nm). Even though primuline is not a species-specific stain, green-stained "capsule-shaped" cysts representing *A. fundyense* were easily and rapidly counted at 10x magnification. The common "egg-shaped" *Scrippsiella* sp. types and "short" cysts, i.e., not as elongated and more round than capsule-shaped, were excluded from the counts. Some stained cysts with no contents may have been counted with this method. These were few in number, however, as empty *A. fundyense* cysts are easily deformed during sonication and sieving and most empty cysts therefore do not have the intact, elongate morphology used as a diagnostic feature for counting.

2.2 Cysts per gram of dry sediment

On some cruises, a replicate 5-cm^3 subsample was removed from the same raw sediment that was used for the corresponding cyst count and placed into a pre-weighed 50-ml centrifuge tube at sea and stored at 4° C. To remove salts before reweighing, 40 ml of deionized water (RT) was added directly to the sediment, mixed, and removed by centrifugation and aspiration of the overlying water and this protocol was repeated. The sample was then dried in an oven at 60° C for at least 72 hours, after which the tube plus sediment was re-weighed. The total number of cysts observed in the corresponding 5-cm^3 subsample was divided by the net weight of the dried sediment to determine the concentration of cysts g^{-1} dry weight (DW).

2.3 Statistical Analysis

2.3.1 Replicate Cores—During each year of the 2007-2011 surveys, six replicate cores were collected at several selected stations to assess sampling variability. Those stations fell within the two subregions (Fig. 1) of the full sampling domain where relatively high cyst concentrations were consistently observed; one station was located in the BOF (122 m-deep) and two were located along the mid-Maine coast (100 m and 123 m depth) in the WGOM subregion. These stations are indicated by larger dots in Figure 2A (2007 panel). The ship relocated within at least 0.2 km of the station coordinates for each redeployment of the corer. Each replicate core was sectioned and processed as noted above. Because these

samples contained relatively high cyst concentrations, approximately 400 cysts could be counted for each layer for each sample, with a corresponding counting error of <10%.

The replicate cores were subjected to one-way repeated measures ANOVA (Systat Software 9.0) with Holm-Sidak pairwise comparisons to test for differences between annual cyst distribution within the 0-1 and 1-3 cm core fractions within and between stations. All data were normally distributed, and therefore were analyzed in their raw form, except cyst abundance data from the 0-1 cm interval within the BOF which required log transformation to achieve normality for this particular analysis. Log-transformation was not required for this data set during all other analyses. Regression analysis was used to investigate a relationship between the number of replicate cores and the coefficient of variance, CV.

2.3.2 Relationship between cysts and bloom metrics—Linear regression analysis was used to examine the relationship between cyst abundance for each survey year and various bloom metrics (e.g., duration and cumulative toxicity of shellfish, km of coastline closed to shellfishing). These analyses were performed using JMP 10.0 (SAS Institute, Cary, NC). Alpha was set at 0.05 for all statistical analyses.

2.4 Definition of a common sampling domain

The area sampled in each large-scale survey changed through time because of weather, bloom distribution, available resources, and scientific objectives. To facilitate comparisons among years with this time series, a common sampling domain was needed. We used the 2009 station map as the common domain as it was the largest area that had the most overlapping coverage among the nine sampling surveys. Within the 2009 domain, we designated three subregions (Fig. 1): The Bay of Fundy (BOF - which includes all stations northeast of Grand Manan Island); the Eastern Gulf of Maine (EGOM – from Grand Manan Island to the midpoint of Penobscot Bay), and the western Gulf of Maine (WGOM – from Penobscot Bay to the southern edge of the 2009 domain). Geographic names and other abbreviations used throughout this text are given in Figure 1. Note that the BOF is considered an integral part of the GOM, treated here as a subregion, similar to the EGOM and WGOM. Note also that our definition of the WGOM is based on the extent of the cyst mapping surveys, and does not include some waters within the western portion of the GOM, such as Massachusetts Bay or offshore waters extending to Georges Bank. The same is true of the BOF, for which the subregion is defined by the sampling area and is not the entire BOF.

Two-sample t-test (Systat Software 9.0) was used to compare mean area (km^2) of the seedbeds (accumulation zones with > 300 cysts cm^{-3}) between the BOF and mid-coast Maine across all years (2004 – 2011).

2.5 Total cyst abundance

Cyst data were gridded onto a high resolution (0.01° latitude) mesh using linear interpolation within Matlab's "meshgrid" and "griddata" algorithms. Subregional cyst abundances were computed by summing the product of each nodal value and its associated area within each of the subregions illustrated in Figure 1.

2.5.1 Scaling the 1997 cyst abundance to the common sampling domain—The sampling domain from 2009 was chosen as the reference area for interannual comparisons. However, since the 1997 survey did not extend as far offshore as in the other years (Fig. 2), it was necessary to scale counts for that year upwards by estimating the number of cysts that would have been present in the unsampled area if the large-scale patterns identified herein were also present during that time. Specifically, the domain sampled in 1997 was compared to the 2009 domain and the unsampled area delineated. The abundance of cysts in that delineated area was calculated for every survey year (2004-2011), and expressed as a percentage of the total cysts observed each year for the WGOM and EGOM subregions for both the 0-1 cm layers and the 1-3 cm layers. The means of these percentages were then used as scaling factors for 1997. In the WGOM, the percentage of total cysts representing the unsampled area was remarkably similar from year to year for the 0-1 cm layer, averaging 18.1% (±2.9 SD) of the amount found in the 1997 domain. For the EGOM subregion, the mean unsampled area 0-1 cm layer percentage was 17.1% (±5.2 SD). For the 1-3 cm layer, the unsampled area contained an average of 18.1% (±6.4 SD) and 16.7 (±7.2 SD) of the cysts in the 1997 domain for the WGOM and EGOM respectively. Thus the 1997 cyst abundance was scaled upwards by factors ranging from 1.17 to 1.18.

The 1997 sampling in the BOF was also more limited in scale than in the other survey years and the station locations differed. Again, due to the importance of 1997 as a year with extremely low cyst abundance, BOF data were scaled to a larger area representative of the other surveys. As the station locations were not the same, however, a slightly different procedure from the one above was used. For the 2004-2011 surveys, stations in close proximity to the 1997 stations were identified and their mean cyst concentration calculated for each sediment layer. A first-order linear regression of the means from these subsamples (n = 6, 1-3 cm; n=7, 0-1 cm) against the means of all stations sampled in the BOF for 2004-2011 (n = 17-24) was highly significant (p = 0.0037), with a slope of 1.25 and coefficient of determination, $R^2 = 0.78$. This relationship made it possible to extrapolate an average cyst concentration for each layer for the BOF in 1997, which when multiplied by the area of the BOF sampling domain (0.43×10^{14} cm^2) yielded an estimate for the total cyst abundance.

2.5.2 Map of mean cyst abundance and variability—A subset of stations that were sampled each year from 2004-2011 was identified by matching locations within 5 km. The time-averaged (arithmetic mean) cyst abundance and associated CV were calculated for co-located station data using the arithmetic mean of replicate samples to represent the station. These statistics are plotted in Figure 3. Data from the 1997 survey was excluded because of the limited areal extent of that survey.

2.6 Characterizing interannual variability in bloom magnitude and extent of PSP shellfish toxicity

There are multiple ways to characterize bloom magnitude, and only some were available or of value in this study. For example, *A. fundyense* vegetative cell concentrations could not be used for year-to-year comparisons, as cruises to obtain cell concentration data during the blooms were not conducted every year, and in those years when they were, temporal and

spatial coverage were not uniform. Large-scale surveys were conducted in 2005, 2006, 2007, 2008 and 2010, with smaller surveys run on an event-response basis in 2005, 2006, 2008, and 2009. A brief summary of *A. fundyense* bloom and toxicity patterns for relevant years is provided in Supplementary Materials A; maps of the *A. fundyense* cell distributions are given in Supplementary Materials B.

In the absence of consistent *A. fundyense* cell concentration data for the study years, we searched for metrics that were available every year and that would reflect either the geographic extent or the intensity and timing of the bloom. The geographic approach utilized data from Kleindinst et al. (this issue) who compiled maps delineating PSP closures for shellfish harvesting in the GOM from 1978 to 2011. From these, the southernmost latitude of PSP toxicity closures in a given year and the total km of coastline closed within the WGOM and EGOM subregions were calculated. Maps for the years before, during, and after each cyst survey year are provided in Supplementary Materials C. Metrics related to the intensity and timing of the bloom are provided by Anderson et al. (this issue). The latter study formulated a HAB Index for the WGOM and EGOM comprised of shellfish monitoring data on bloom duration, number of stations with detectable toxicity, and cumulative toxicity. These were tabulated for each year from 1978 to 2011 to provide an integrated measure of bloom severity.

Where shellfish harvesting closures are used as the metric, the bloom is characterized on the basis of toxicity scores approaching or exceeding 80 μg saxitoxin equivalents (STX eq.) 100 g^{-1}, the regulatory limit for PSP toxicity in bivalves for human consumption. When duration or termination of toxicity are utilized as metrics, the bloom is characterized in terms of detectable levels of toxicity which are ~40 μg STX eq. 100 g^{-1} using the mouse bioassay. Bloom termination date is defined as the date at which there is no longer detectable toxicity at any station within the EGOM+WGOM subregions.

There are a number of caveats associated with these bloom descriptors, and as a result, care must be taken in making inferences about bloom dynamics based on coastal shellfish toxicity metrics. First, the cell concentrations necessary to make shellfish toxic are quite low in the region, ca. 200 cells L^{-1} (Keafer et al., 2004). Because *A. fundyense* concentrations can vary up to several orders of magnitude above that threshold, the "bloom duration" and "bloom termination" inferences made from shellfish toxicity measurements in nearshore coastal waters do not resolve the full dynamic range of regional populations. Moreover, *A. fundyense* population dynamics in the region are driven primarily by offshore phenomena, and the exposure to shellfish beds depends heavily on hydrodynamic transport of toxic cells to inshore waters (Franks and Anderson, 1992a; Anderson et al. 2005a; McGillicuddy et al., 2003, 2005). Therefore, shellfish toxicity in nearshore waters does not necessarily reflect the size of the offshore *Alexandrium* populations.

2.7 Relationship between cyst abundance and metrics of preceding and successive bloom magnitude or extent

Possible linkages between cyst abundance and a variety of bloom metrics (discussed above) were examined. Regressions were run between *A. fundyense* cyst abundance (determined in the fall of each survey year) and the geographic extent or severity of the bloom the

following year. For convenience, we refer to these relationships as *cysts → blooms*. In a similar manner, relationships were examined between the severity or geographic extent of blooms and the subsequent cyst abundance later that same year. This is referred to as *blooms → cysts*. We acknowledge that without vegetative cell abundance data, the "blooms" term is not exactly correct, but is less cumbersome than the alternative of using multiple terms such as *cysts → closures, cysts → toxicity*, or *closures → cysts, toxicity → cysts*, etc.

3 Results

3.1 Measures of cyst abundance

Two measures of cyst abundance were assessed in this study. For one, cysts were enumerated and the concentration expressed in terms of the wet volume of the raw sediment (cysts cm^{-3}) while for the other, the cyst counts were normalized to the dry weight of the sample (cysts g^{-1} dry weight). These dual analyses were conducted for 85 stations during the 2005 cyst survey, with each analysis being performed for both 0-1 and the 1-3 cm layers. Thus a total of 170 analyses were run in parallel, 85 at each depth of sediment. This covered all major cyst accumulation areas, as well as areas with low cyst abundance, and thus widely different depositional and erosional environments.

Figures 4A, B show contour maps of cyst concentration using these two metrics. For comparison purposes, the scales for the figures have been adjusted so that the highest values approximately correspond to the same color. (Note that Figure 4A differs from the 2005 map presented in Figure 2A because the former shows a subset of stations for which both enumeration methods were carried out.) It is clear that each of these enumeration methods delineates the same seedbeds and low abundance zones in the regional cyst distribution.

The quantitative relationship between these two cyst enumeration metrics is shown in Figure 4C for the 0-1 cm sediment layer, and Figure 4D for the 1-3 cm layer. In both cases, a significant positive linear relationship is evident ($p < 0.0001$), with R^2 values of 0.82 and 0.96 respectively. The slopes of the two regressions are also similar, indicating that a consistent, direct and quantitative relationship exists between cysts expressed per unit volume or per-unit DW for the GOM. Accordingly, for the remainder of this paper, we will describe the abundance of cysts using cysts cm^{-3}, as this permits many important calculations and analyses that are not possible with dry weight determinations, unless concurrent measurements of sediment bulk density are made, as detailed below.

3.2 Variability among Replicate Cores

Multiple cores (6 replicates) were collected at three stations each year from 2007 – 2011 to explore the inherent variability in cyst abundance in the 0-1 cm and 1-3 cm core sections at each station each year (Fig. 5). Overall, cyst abundance was slightly more variable in the upper 0-1 cm layer of the cores relative to the lower 1-3 cm layer, with mean CVs of 0.42 and 0.36, respectively.

At all other stations in each mapping survey, only one core was taken per station per year. Given a fixed amount of ship time, this increased the geographical range of cores taken compared to the alternative, which would be to collect replicates at fewer stations. If we had

increased the number of cores taken at each station from 1 to 3 to capture more variability at each station, the CV would have only decreased by a factor of 1.7, as the CV for an average of n cores varies inversely with n. It was, therefore, decided that an expanded geographical range was more important for the overall modeling efforts than reducing variability around the sampling mean by sampling half as many stations with replicates, or one-third as many in triplicate.

3.3 Large-scale cyst surveys

Maps of cyst abundances in the surface sediment (0-1 cm) for each of the survey years are shown in Figure 2A, and cyst abundances for deeper (1-3 cm) sediment are shown in Figure 2B. Cyst concentrations at individual stations were highly variable, with values ranging from 0 to 6,700 cysts cm^{-3} in the surface layer (= 67 million cysts m^{-2} in the top 1 cm of sediment). The multi-year mean cyst distribution (Fig. 3), derived from eight large-scale cyst surveys (2004-2011), show two well-defined accumulation zones or seedbeds, one in the BOF and the other offshore of mid-coast Maine. These seedbeds are within a broad distribution that spans over 600 km in the alongshore direction and at least 150 km in the offshore direction. Cysts are found in low abundance between the BOF and the mid-coast Maine seedbed, and between that seedbed and Massachusetts Bay and other coastal waters to the south and west. Within the WGOM and EGOM, the offshore seedbeds lie deeper than the 75-m isobath, with dense cyst accumulations at ≧150 m. The cyst distribution appears broader for the 1-3 cm depth interval (Fig. 3B) compared to the 0-1cm interval (Fig. 3A), extending farther southwestward along the Maine coast from the BOF and farther offshore from the mid-Maine coast seedbed. In addition, the mid-coast Maine seedbed extends farther northeastward in the deeper sediment layer.

The variability in surface layer (0-1 cm) cyst abundance depicted in the mean map (Fig. 3C, D) is highest in the western sections of the sampling domain and in the BOF to the east of Grand Manan Island. The CV of the 1-3 cm layer is less than that of the 0-1 cm layer, especially in the two major seedbeds.

In general, the largest cyst populations in the GOM are found in the area of fine silt and clay and M_2 tidal currents less than about 10 cm s^{-1} (Butman et al., this issue). However, there are regions of fine-grained sediment where the minimum tidal current is less than this level and cysts are not found in abundance, suggesting that the supply of cysts to those regions is limited by the bloom dynamics and regional circulation.

The geographic extent or area of the seedbeds (arbitrarily defined as the area within the 300 cysts cm^{-3} contour) varied 3-4-fold among years (Fig. 2A,B; Table 1). In western Maine, 2006 was the smallest (5,634 km^2) and 2007 the largest (19,393 km^2). In the BOF, 2011 was the smallest (1,108 km^2) and 2009 the largest (4,383 km^2). The mean size of the seedbed in the WGOM subregion (12,412 km^2 ± 5,307 SD) was significantly larger than the mean of the seedbed area in the BOF (2,292 km^2 ± 1,102 SD) when averaged over all years (p < 0.001, t = 5.281, df = 14). The 1997 survey is not included in the calculations due to the smaller size of the sampling domain.

Significant interannual variability in total GOM cyst abundance is evident across the nine surveys (Figs. 2A,B, 6). Table 2 shows how the cyst abundance for each year compares to the arithmetic mean cyst abundance baseline level, hereafter termed "mean cyst abundance". Values are expressed as the total number of cysts in a given sediment layer for each GOM subregion, and the percent change relative to the mean cyst abundance. In the WGOM, for example, 2009 surface layer cyst abundance was nearly double the mean, whereas 1997 was approximately one-fifth of the mean. Thus, 2009 was more than 10 fold higher than 1997. In the EGOM, the 2007 surface cyst abundance was 1.5x the mean, whereas the 1997 levels were < one-fifth of the mean. Another relatively low abundance year was 2011 which had one-half of the mean cyst abundance in all three GOM subregions. Similar patterns are apparent for the 1-3 cm layer, with 2005 and 2009 emerging as the highest years for the WGOM (1.9 and 1.1 × higher than the mean cyst abundance) and EGOM (1.9 and 1.4 × higher than the mean respectively).

These patterns are illustrated in Figure 6. It is evident that at the surface, the years with high cyst abundance were 2004, 2007, 2009, and 2010 (Fig. 6A), whereas for the 1-3 cm subsurface layer (Fig. 6B), the high years were 2005, 2009, and 2010. For the total (0-3 cm; Fig. 6C), the high years were 2005, 2007, 2009, and 2010.

The WGOM subregion had the highest average surface (0-1 cm) cyst abundance at 12.2×10^{16} cysts cm^{-3} (± SD 9.2), followed by the EGOM at 3.4 cm^{-3} (±1.6) and the BOF at 2.1×10^{16} cysts cm^{-3} (± 1.3) (Tables 2, 3). The WGOM (effectively, the mid-coast Maine seedbed) thus holds nearly 2/3 of the *A. fundyense* cysts in the GOM.

The concentration of cysts was slightly higher in the deeper sediment layer than the surface. The abundance of cysts in the 1-3 cm layer relative to the total cysts in 0-3 cm for all three domains over all survey years ranged from 71.2% to 77.5% (Table 4). The percentages of cysts in the surface layer were 28.8, 22.5, and 27.7 for the WGOM, EGOM, and BOF respectively. Since the 1-3 cm layer is 2-cm thick, the mean quantity in each cm of that layer ranged from 35.5 to 38.8% of the total.

For most survey years, the geographic focus was the coastal and central portions of the GOM, but in 2007, Georges Bank was also surveyed (Fig. 2; McGillicuddy et al., this issue-b). Cysts were undetectable or in very low abundance (0-25 cysts cm^{-3}) at most stations, with slightly elevated abundances (50-100 cysts cm^{-3}) along the southern flank of the bank, but still well below the levels seen elsewhere in the GOM.

A southward expansion of the mid-coast Maine cyst seedbed was observed following the 2009 bloom. This bloom, discussed in detail in McGillicuddy et al. (this issue-a), included a large "red-water" patch of *A. fundyense* near Portsmouth, New Hampshire, observed in mid-summer, that was associated with anomalously high cyst fluxes observed downstream of that area (Pilskaln et al., this issue-a). That autumn, the annual cyst survey revealed a major extension of the mid-coast Maine seedbed to the south, primarily reflected in a band of high cyst abundance east of Cape Ann in the 0-1 cm interval (Fig. 2A). By the autumn of 2010, however, the cysts were no longer abundant there, with the distribution reverting to the pattern seen every year since 2004 (Fig. 2A,B). Figure 7 shows a time series of cyst

concentrations at two stations located within the area of the 2009 seedbed expansion (stations MB-7 and MB-12, identified in Fig. 2A for 2009). In 2008, before the red-water event, cysts were scarce in both the surface and 1-3 cm layers at both stations, consistent with past surveys in that area, whereas in 2009, *A. fundyense* cyst concentrations were very high at both stations. Notably, at MB-7, surface mean cyst concentration was 5x higher than in each cm of the 1-3 cm layers (Fig 7A), and at MB-12, surface cyst concentration was 43x higher than at the lower layers, consistent with the deposition of new cysts from the red-water bloom three months earlier. Targeted sampling in June 2010 showed that *A. fundyense* cysts were essentially back to the scarce 2008 levels in both the surface and 1-3 cm layers (Fig. 7).

3.4 Relationship between cyst abundance and successive blooms

The relationship between cyst abundance in autumn and measures of the bloom in the following spring (*cysts → blooms*) is explored in Figures 8-10. The independent variable is taken to be cyst abundance, and the dependent variable is length of coastline closed to shellfish harvesting or latitude of southernmost closure. Figure 8 shows linear relationships between cyst abundance and the length of coastline closed due to PSP toxicity the following spring. In Figure 8A, a positive relationship is suggested but is not significant (p = 0.0568) between 0-1 cm layer cyst abundance in the WGOM+EGOM subregions and the km of coastline closures the following year in the same two subregions. If total (0-3 cm) cysts are used in these analyses, the relationship is significant (Fig. 8B; p = 0.0374). If WGOM +EGOM cysts are regressed against only the WGOM coastline closure length, the relationships are significant with both surface 0-1 cm (Fig. 8C; p = 0.0160) and total 0-3 cm cysts (Fig. 8D; p=0.0222). None of the above regressions include 2009 cysts or 2010 bloom extent, as 2010 was an anomalous year in which the *A. fundyense* bloom was suppressed by a regional water mass anomaly, as discussed below and in McGillicuddy et al. (2011). The extent to which 2010 deviates from the patterns established by all other years is evident in Figure 9, which shows the relationship between fall cyst abundance (0-1 cm) in the WGOM and the latitude of the southernmost closure due to PSP toxicity for the following spring in each of the study years. This is an updated version of the figure presented by McGillicuddy et al. (2011) through the addition of the bloom years of 1998, 2011, and 2012. The strong and significant positive relationship first reported by those authors is confirmed by regression analysis of the expanded data set (Fig. 10C; p = 0.0023).

We also examined the relationship between WGOM+EGOM 0-1 cm cyst abundance and latitude of the southernmost closure the next year and found a significant correlation (Fig. 10A; p = 0.0020). If the total 0-3 cm cyst abundance is used in these analyses for the WGOM+EGOM (Fig. 10B) and WGOM only (Fig. 10D), both relationships are significant (p=0.0422, and 0.0220, respectively). Here again, if 2010 is included, the R^2 values decrease markedly, ranging from 0.00 to 0.11 for Figure 10A-D, and none of the relationships are significant, with p values ranging from 0.3719 to 0.9764.

Looking to measures of bloom intensity rather than geographic extent in this *cysts → blooms* analysis, regressions were not significant between WGOM+EGOM surface (0-1 cm)

and total 0-3 cm cyst abundance and the WGOM+EGOM cumulative shellfish toxicity per station or duration of detectable toxicity (Table 5), as defined in Anderson et al. (this issue).

3.5 Relationship between blooms and subsequent cyst abundance

The relationship between the geographic extent and intensity of a bloom in a given year and the abundance of *A. fundyense* cysts measured later that same year (*blooms → cysts*) is explored in Figures 11 - 14. In these cases, the independent variable is taken to be a metric of coastal shellfish toxicity indicative of bloom extent or intensity, and the dependent variable is cyst abundance. Data for 2010 are included for this analysis because we know of no reason why the water mass anomaly that suppressed the bloom that year (McGillicuddy et al., 2011) would also affect the encystment process.

No statistically significant linkage was observed between either the length of coastline closed in a given year or the latitude of the southernmost closure and the abundance of *A. fundyense* cysts in the surface 0-1 cm layer for any subregion or combination of subregions (Table 6). A significant relationship was observed between the extent of EGOM coastline closures and cyst abundance in the top 3 cm of sediment in the WGOM+EGOM subregions (Fig. 11; p = 0.0246).

Regressions between metrics of bloom intensity such as cumulative shellfish toxicity and duration, and the surface layer 0-1 cm cyst abundance measured later that year yielded no significant relationships, with the exception of bloom (toxicity) termination date. In that analysis, significant relationships were observed between WGOM+EGOM cyst abundance and bloom termination date using both the surface (Fig. 12A; p=0.0277) and the 0-3 cm layers (Fig. 12B; p=0.0112).

Another metric used here and in the derivation of a HAB Index used to characterize the overall severity of *A. fundyense* blooms in the WGOM and EGOM regions (Anderson et al., this issue) is the average cumulative shellfish toxicity per station (calculated for the 160 shellfish monitoring stations in Maine) for each year. For this descriptor, toxicity measured in mussels (*Mytilus edulis*) is summed over the bloom season for all stations and sampling times, and divided by the number of stations reporting. This allows a cumulative toxicity metric to be calculated separately for the WGOM and the EGOM subregions as they have different numbers of shellfish monitoring stations. The relationship between this metric and WGOM+EGOM 0-3 cm cyst abundance is significant (Fig. 13; p = 0.0085). The relationship between 0-3 cm cyst abundance and the duration of the preceding bloom was also examined and is significant (Fig. 14; p = 0.0084). Here, duration is defined as the interval between the first detection of toxicity at any station in the subregion and the last measureable toxicity at any station (Anderson et al., this issue).

Note that duration information is only available for the state of Maine, since Massachusetts and New Hampshire do not have records as far back as Maine, nor do they have historical records of duration. However, analysis of shellfish toxicity data for the years in which that information is available for all states in the region indicate that harvesting closures were always initiated first and terminated last in Maine (Kleindinst et al., this issue). Thus, duration and termination information from closures in Maine may be considered

representative of the WGOM+EGOM subregions (that is, including New Hampshire and Massachusetts).

4 Discussion

Numerous studies have enumerated cysts for a wide range of habitats and dinoflagellate species, identifying seedbeds and linking these to blooms (e.g., Anderson and Morel, 1979; Genovesi et al., 2009; Crespo et al., 2011; Ni Rhataille and Raine, 2011; Angeles et al., 2010, 2012; Martin et al., this issue). Few, however, have studied the dynamics and evolution of those seedbeds over multiple bloom cycles and years. Here we document cyst abundance and distribution patterns over nine years in the coastal waters of the GOM and identify linkages between those patterns and several metrics of *A. fundyense* bloom geographic extent and intensity (inferred from coastal shellfish toxicity records) in the years immediately before and after each cyst mapping survey. Linkages are identified between cyst abundance and subsequent blooms, and between blooms and subsequent cyst abundance. Furthermore, we explore the relative utility of different measures of cyst abundance in bottom sediments, and demonstrate that GOM cyst abundance can be normalized to sediment volume, contrary to the claims of those who argue that cysts g DW^{-1} is the only suitable measure (Dale, 2000; Matsuoka and Fukuyo, 2000). These and other topics are discussed in more detail below.

4.1 Quantitative measures of cyst abundance in bottom sediments

Surveys of the distribution and abundance of cysts are clearly useful in ecological and monitoring studies of HABs and shellfish toxins, and quantitative studies of dinoflagellate cysts in ocean sediments have also been conducted by paleontologists for many years. Typically, the latter investigations enumerate cysts at different depths in sediment cores, expressing the results in terms of cysts g DW^{-1} sediment (e.g. Lee and Matsuoka, 1994; Cho and Matsuoka, 1999). This unit has been selected because there are different degrees of compaction and thus water content in a core (Dale, 2000; 2001). Although this approach is appropriate when one is studying vertical profiles of dead, empty, or fossilized cysts in sediments dating back hundreds or thousands of years, it provides limited information to ecologists investigating the dynamics of living cysts in surface sediments, as in this study. Many have interpreted Dale's (2000) recommendation that "future studies use standardized methods based on measurements of cyst concentrations per gram of dry sediment" as a guideline to be followed in all investigations of cyst abundance or dynamics – ecological or paleontological. Indeed, this contention has been supported in training manuals for those working with living dinoflagellate cysts (e.g. Matsuoka and Fukuyo, 2000). The argument has been that the water content and lithology of surface sediments differs sufficiently from site to site, or from layer to layer, and that normalization of cyst abundance to a volume of sediment introduces substantial errors compared to the dry weight approach (Dale, 2000). The argument is also made that the flocculant or "fluffy" nature of surface sediments makes the surface layer difficult to sample and thus that volume measurements are uncertain or inaccurate.

One of the objectives of our research programs in the GOM has been to understand the distributional dynamics of *A. fundyense* cysts (Anderson et al., 2005d) and to develop numerical models of *A. fundyense* population dynamics that can be initiated from the cyst survey maps presented here. However, in order to calculate an inoculum, the number of cysts per unit area of ocean bottom must be known. In our modeling studies (e.g., McGillicuddy et al., 2003, 2005, 2011; Stock et al., 2005; He et al., 2008; Li et al., 2009) we have taken the cyst cm^{-3} of sediment data shown in Figures 2A,B and assumed that the bloom inoculum originates from germination within the 0-1 cm layer of sediment. The units of concentration (cysts cm^{-3}) allow a simple calculation of cysts m^{-2} of ocean bottom, which is then used to generate a time-varying flux of newly germinated cells into the water column, with germination rates based on laboratory measurements (Anderson et al., 2005c; Stock et al., 2005). A similar flux could not be calculated over large areas with different sediment types if cyst abundance is calculated per g DW^{-1} unless conversion factors are provided relating mass to volume (e.g., density) across stations.

To address criticisms that expressing cysts per unit volume is potentially inaccurate or misleading, core samples were processed two ways during our 2005 survey. This yielded cyst abundance estimates per unit DW and per unit volume of sediment. It is evident in both the areal distribution of cysts (Figs. 4A,B) and from the first-order regressions for the 0-1 cm and 1-3 cm layers (Figs. 4C,D) that there is an extremely tight correlation between these two different measures of cyst abundance in the surface sediments of the GOM. With highly significant correlations representing data from a broad range of surface sediment types (85 stations, two layers analyzed at each) it is evident that cysts cm^{-3} of sediment is a meaningful and consistent unit of measure for studies of *A. fundyense* cyst dynamics in the GOM region. It remains to be determined whether cyst abundances expressed per unit volume can be compared across geographic regions given differences in sediment characteristics and collection methods, but within a given region, we recommend that other workers conduct comparative studies to justify the use of this approach. We hope that those working on dinoflagellate cysts recognize the validity and value of the two different approaches for cyst enumeration – cyst number g DW^{-1} for paleontological reconstructions of past populations and sediment transport modeling, and cysts per unit area or unit volume for studies of the dynamics of living cysts. Another option would be to measure cysts g DW^{-1} and also determine the density of each sediment layer, as this would allow a simple calculation that would also provide cysts per unit volume data.

4.2 Variability among replicate cores

In planning the stations to be sampled for the cyst-mapping surveys, a difficult trade-off was faced between providing the largest geographic coverage within the allotted ship time and adequately addressing patchiness and small-scale variability in the underlying cyst distribution. We chose to collect single cores at each of the 100+ stations for the broad-scale surveys, while also obtaining replicate cores allowing more detailed statistical analysis, from three selected stations to estimate small-scale variability (Fig. 5). In these latter analyses, the average CV of all replicates was ~40%, with individual replicates differing by a factor of two or more at a given station at a single point in time. While there was thus a significant amount of uncertainty in each point estimate of cyst abundance, replicate cores were not

necessary to decipher large-scale trends, as definitive spatial structure was persistent year to year (i.e., each station is surrounded by others that provide spatial continuity to the estimates). Replicates would only have been of benefit if there was more variability within a station than among stations, which was not the case based on our in-depth analysis of the three stations and multiple years of broad-scale surveys.

4.3 Vertical cyst distribution and bioturbation

Vertical profiles of living dinoflagellate cyst abundance in surface sediments show considerable structure with depth (Anderson et al., 1982; Keafer et al., 1992), as each profile represents the net result of biological processes such as cyst deposition, germination, bioturbation, and mortality, as well as physical processes such as mixing, sedimentation, and resuspension. The variability in these processes through time and between locations will have a significant impact on the cyst abundance measurements in surveys, particularly since blooms differ dramatically in their termination date (Anderson et al., this issue), and thus in the most likely timing of mass cyst formation and deposition. For the nine years of this study, termination date ranged from 14 July (1997) to 5 November (2009) (Anderson et al., this issue), i.e., a difference of nearly four months.

A study by Keafer et al., (1992) explored bioturbation, sedimentation, and other burial and mixing processes in GOM sediments within the WGOM subregion. They used ^{210}Pb to document a dynamic zone of rapid bioturbation 2-6 cm thick above another region (6 to at least 12 cm thick) in which mixing was slower but still dominant over sedimentation. These workers also formulated a model to demonstrate that a pulse deposition of cysts from a bloom would be mixed over depths of 0-5 cm within a few months of the event. Cyst abundance decreased with depth within and below that layer, with some cysts remaining near the surface as a potential inoculum for the next year's bloom. In a related study, Shull et al. (this issue) obtained profiles of cysts, O_2 and benthic infauna on several occasions between September 2003 and August 2005 at a site within the WGOM subregion, and used these data with ^{210}Pb dating to develop a benthic mixing model. In summer, observed cyst concentrations increased from near zero at the sediment surface, reaching a subsurface maximum between about 10 to 15 cm, and then declining in abundance with depth. One exception was the August 2004 sample which showed surface enrichment in cysts (possibly due to a late-season bloom – see Supplementary Materials A). Shull's mixing model predicted the subsurface maximum (caused by benthic organisms that ingest at the surface and egest at depth), and that some of the cysts deposited at the end of the bloom would remain at the sediment surface over the late fall and winter, when mixing is insufficient to completely transport these recently deposited cysts downward. These cysts are then available to germinate the following spring. We note that Butman et al. (this issue) found some suggestion of very near-surface enrichment in late fall 2011 samples.

In recognition of processes involving cyst mixing and burial, we tabulated cyst inventories over the 0-3 cm layer, but broke this into two intervals – the surface 0-1 cm layer, and the lower, 1-3 cm layer. For some analyses, these layers were combined into a single 0-3 cm total. We acknowledge that some newly deposited cysts might be buried below this layer in the few months that typically separated bloom termination from the cyst survey and thus

would not be counted, but based on the model presented in Keafer et al. (1992) we suggest that number is small relative to those in the 0-3 cm layer.

We separated the surface 0-1 cm layer from the 1-3 cm layer below because most cyst germination occurs from that top layer due to the absolute requirement of oxygen for germination of dinoflagellate cysts (Anderson et al., 1987). In the Keafer et al. (1992) study, direct measurements showed detectable oxygen down to 1 cm. In a study by Shull et al. (this issue), oxygen and autofluorescent cysts were detected down to 1.5 to 2 cm in the mid-coast Maine seedbed.

We are therefore faced with a conundrum in our efforts to inventory cysts and establish relationships between cyst abundance and various bloom parameters. When cysts are formed by blooms, they fall to the sediments and are buried and mixed, so when we explore *blooms → cysts* linkages, there is good reason to inventory the 0-3 cm layer, particularly with the observed 4-month range of bloom termination dates. Indeed, this approach gives the strongest relationships between bloom metrics and resulting cyst abundances. However, for linkages between cyst abundance and the subsequent bloom (*cysts → blooms*), we focused on the 0-1 cm oxygenated upper layer, from which recently germinated cells can potentially access the overlying water column. The surface cm is located at the top of a thicker, dynamic sediment layer in which cysts are moved both upwards and downwards primarily due to animal burrowing and feeding activity (see Shull et al., this issue). One might therefore argue that it is more appropriate to use that entire 0-3 cm layer, or some fixed proportion of it (see section 3.5) in *cysts → blooms* analyses, given the lack of knowledge of downward versus upward mixing rates from, or into, that surface cm. However, we do describe significant relationships between cyst abundances in both the 0-1 cm and the 0-3 cm layers and a variety of metrics of the geographic extent for the subsequent blooms (e.g. Fig. 8B-D and Fig. 10A-D). Furthermore, we have demonstrated skill in model simulations initiated from that 1-cm surface layer when compared with cruise survey data from multiple years (He et al., 2008; Li et al., 2009, this issue; McGillicuddy et al., 2011). We therefore infer that concentrations in the top cm are a reasonable proxy for the number of cysts available for germination the following spring, assuming that factors influencing germination rates and mixing of surface sediments have remained fairly constant over the years.

4.4 Cyst distribution patterns

The WGOM subregion, which includes the mid-coast Maine seedbed, always contained the highest inventory of cysts, with average annual totals that were 2.6 times higher than those in the EGOM, and 5.5 times larger than the BOF. The WGOM and EGOM subregions are approximately equal in area and each is 4-5 times larger than the BOF (Table 1). Thus mean cyst concentrations per unit area are comparable in the WGOM and the BOF, and approximately twice those in the EGOM. One explanation for the relative scarcity of cysts in the EGOM is provided by McGillicuddy et al. (2005), who argue that nutrient limitation in the MCC is more prevalent in the WGOM than in the EGOM during *A. fundyense* blooms. Nutrient limitation is considered a major factor in cyst formation in *Alexandrium* (Turpin et al., 1978; Anderson and Lindquist, 1985; Anderson et al., 1994).

Alexandrium fundyense cysts are not uniformly distributed within the subregions. Two distinct seedbeds are evident (Fig 3A,B), flanked by regions with markedly lower cyst abundance. One seedbed is located in the BOF and a much larger one in the WGOM, consistent with those identified by Anderson et al. (2005c). The areas of these seedbeds varied 3-4 fold among years, although their general location did not change. Smaller-scale features within these seedbeds are also evident (Fig. 2) such as lobes of the mid-coast Maine seedbed, or the extension of that seedbed towards the BOF along the pathway of the nearshore portion of the eastern segment of the MCC. The mean cyst map for the 1-3 cm layer (Fig. 3B) suggests a broader and more persistent deeper reservoir than the surface layer (Fig. 3A).

These seedbeds appear to reflect the transport pathways of the coastal currents in the region. Thus the BOF cyst accumulation zone (Martin and White, 1988; Martin et al., this issue) lies below the recirculating gyre found at the mouth of the BOF (Aretxabaleta et al., 2008, 2009), as would be expected if cysts formed during the blooms in those waters eventually accumulate in bottom sediments. The mid-coast Maine seedbed broadens in the offshore direction south of Penobscot Bay, consistent with the veering offshore of the MCC. This hydrographic feature, which has been described by Pettigrew et al. (2005) and others, is associated with offshore transport of *A. fundyense* populations in that area (Townsend et al., 2001). It follows that cysts formed by those populations might fall into the WGOM offshore zone as the MCC veers to the south and away from shore. This feature is visible in all years (see Fig. 3A,B), but is especially evident in 2004, 2007, and 2011 (Fig. 2A,B). Evidence of a continuation of that offshore veering pathway is also visible, suggesting transport of cells and cysts northward around the eastern edge of the Jordan Basin gyre (Fig. 2, 2008; Fig. 3A,B). At times when the alongshore direction of the MCC flow is dominant, cysts may settle farther to the south and west (Fig. 2, 2009).

Over the study period, the two major seedbeds are relatively persistent geographic features, although varying in size and cyst abundance. The regional system thus seems to have only two seedbeds, areas where the bathymetry, sediment characteristics, currents, and biology are suitable for high cyst inventories to persist for decades or longer. We suggest that the majority of cysts formed in the areas south and west of the mid-coast Maine seedbed are dispersed over broad areas and not retained within discrete seedbeds. Furthermore, we suggest *A. fundyense* populations that cause closures in that region do not contribute cysts to the inventory of the two major seedbeds that are upstream in the MCC.

Our mapping of seedbeds and areas with low cyst abundance (Fig. 2A,B) suggests that it may be possible to reduce the number of stations occupied in the cyst surveys and still obtain an estimate of cyst abundance useful for bloom prediction. The resources required for the mapping surveys are considerable and need to be reduced if the *A. fundyense* population dynamics model is to be applied for operational forecasting of HABs in the region, as is planned. Reduced sampling could be accomplished by using the time-series data (Fig. 2A,B) to build a statistical model of a generic GOM cyst distribution pattern that can be scaled upwards or downwards with data from a subset of sampled stations. This would make it possible to extrapolate a limited number of cyst abundance observations to an overall GOM cyst inventory. We have applied this concept by using the data from 2004 – 2011 to estimate

the number of cysts that were not sampled in the offshore area outside the 1997 survey domain but within the 2009 domain (termed the 'unsampled' area). The percentage of total cysts found in the unsampled area was remarkably similar from year to year, averaging 18.1 and 17.1% for the WGOM and EGOM respectively. Likewise, a similar extrapolation of a limited number of stations sampled in 1997 to a full BOF subregion estimate for that year was statistically justified (see Methods).

Development of a statistical model of the GOM cyst distribution is underway (A. Solow, pers. comm.) and thus far, it does appear that a generic distribution exists and that a smaller number of stations can be sampled and results extrapolated. As promising as this sampling reduction strategy appears, it is essential that periodically, large-scale cyst maps be obtained to ensure that major changes would be detected, such as the brief extension of the mid-coast Maine seedbed in 2009 (McGillicuddy et al., this issue-a).

4.5 Variability in cyst abundance

Significant interannual variability in total GOM cyst abundance is evident from the nine surveys (Fig. 2). Most of the variation was controlled by the cyst abundance in the WGOM (Fig. 6), as reflected in higher CV values for the mean cyst map (Fig. 3C,D). Analysis of the long-term variability at individual stations (Fig. 3C,D) shows that year-to-year differences are highest at the fringes of seedbeds in the WGOM and in the BOF, and in some cases are defined by one location. These geographic differences could reflect small-scale spatial variability (Fig. 5) within the 5-km averaging window. In the WGOM, the high CV values offshore of New Hampshire and northern Massachusetts appear to reflect the sudden appearance (2009) and disappearance (2010) of the mid-coast Maine seedbed extension in an area that had very low cyst abundance in all other years.

Table 2 contains a compilation of GOM cyst abundance data collected during 1997 and 2004-2011. To complement this dataset, we note that Martin et al. (this issue) counted cysts in the surface layer of the BOF in the early 1980s. For the BOF subdomain, as defined here, we calculate the cyst inventories for 1981, 1982, and 1983 to be 2.0, 2.0, and 2.1×10^{16} total cysts, respectively. These values fall into the general range in the BOF for other years of this study from 2004 – 2011 (Table 2).

Cyst surveys were limited on Georges Bank, but samples taken there in 2007 showed that *A. fundyense* cysts were undetectable or in low abundance at most stations (Fig. 2A, B). Despite this low cyst abundance, Georges Bank can be the site of large *A. fundyense* blooms (McGillicuddy et al., this issue-b). The retentive circulation and favorable growing conditions on the bank were suggested as being responsible for the development of a small initial inoculum into substantial populations, but it is not known whether the inoculum was from the sparse cysts located in the bank's sediments, or from cysts or cells in adjacent waters that wash onto the bank and germinate or grow there. In either case, *A. fundyense* bloom dynamics are thought to be controlled by the balance between growth and mortality on the bank and not cyst abundance.

4.6 Cyst abundance as a determinant of bloom geographic extent and intensity

Many studies have argued that the number of cysts in an area is important for bloom initiation, but for certain systems is not a major determinant of bloom magnitude, as indicated by maximum cell concentrations (Anderson, 1998; Anderson et al., 1983; Angeles et al., 2012; Hattenrath et al., 2010). In those studies, most have typically focused on shallow, relatively enclosed habitats with reduced water exchange, so the factors that regulate cell division tend to dominate over the relatively small and gradual cyst germination inoculum. This is not the case in the GOM, however, as numerous studies (e.g., Li et al., 2009; this issue; McGillicuddy et al., 2005; 2011) support the hypothesis that cyst abundance can be considered a first-order predictor of regional bloom severity the following year, with the important caveat that other factors will determine the extent of population growth and delivery to shore (McGillicuddy et al., 2011).

Several features of the GOM system might explain this relationship. First, with the exception of the BOF, *A. fundyense* vegetative cell concentrations are generally quite low in the region (low thousands L^{-1}; Supplementary Materials B). Occasional densities of 50,000 cells L^{-1} (Townsend et al., 2001; Anderson et al., 2005b) are observed and on very rare occasions, concentrations exceed 1×10^6 (McGillicuddy et al., this issue-a). Thus, the size of the initial germination inoculum may be comparable to the eventual bloom size achieved through cell division. For example, if all cysts in the 0-1 cm sediment layer with a concentration of 1,000 cysts cm^{-3} germinated and swam to the surface, this would give a vegetative cell concentration of 1,000 cells L^{-1} in the top 10 m of the water column. In contrast, similar cyst concentrations in the shallow embayments mentioned above can lead to blooms with millions of cells L^{-1}, many times larger than the initial inoculum (Anderson, 1998; Hattenrath et al., 2010; Crespo et al., 2011; Angeles et al., 2012).

The relative constancy in the location of the *A. fundyense* cyst seedbeds may be another factor in support of this relationship. The seedbeds change in size from year to year (Fig. 2A,B), but remain in the same general locations, which allows the cells to emerge and enter surface waters in much the same location and time every year, providing a level of continuity in the annual PSP outbreaks.

Cyst abundance was not correlated with every metric of the subsequent bloom, however. For example, cyst abundance (in both the surface cm and 0-3 cm layers) in any subregion or combination of subregions, was not correlated with the following year's duration of toxicity or the cumulative toxicity per station. This lack of correlation may be because bloom duration and cumulative toxicity are metrics that are more affected by environmental factors such as nutrients or wind patterns than are coastline closures. As discussed earlier, the latter are simply determined by a threshold toxicity level. In a similar manner, Martin et al. (this issue) found no link between cyst abundance and the magnitude (cell abundance) of subsequent *A. fundyense* blooms in the BOF. No geographic metrics were tested in that study.

In the GOM, when the subsequent year's bloom is categorized on the basis of total length of coastline closed, significant relationships emerge with the size of the preceding year's cyst inventory. Abundances from the WGOM+EGOM subregions were linked with WGOM

+EGOM closure length (Fig. 8B) and with WGOM closure length (Fig. 8C,D). Clearly, cysts that are 'upstream' of an area are most closely linked to the length of subsequent closures within and downstream of that area, i.e., EGOM cysts contribute to WGOM blooms given the directional nature of the MCC transport pathway.

An even stronger relationship was observed between cyst abundance and the latitude of the southernmost closure the next year when the surface 0-1 cm layer was used (Fig. 10A,C). First-order regressions were significant for all the tested subregion combinations (Fig. 10A-D). Again, this finding is consistent with the view that the southernmost closure reflects the combined effects of subregional populations of *A. fundyense* in the alongshore MCC transport pathway.

Summarizing the *cysts → blooms* analyses, we identified several strong relationships between surface 0-1 cm and total 0-3 cm cyst abundance and the geographic extent of the GOM blooms. These are important findings from a management perspective, as cyst maps are shown to have value for seasonal bloom predictions, either through the application of a numerical model (e.g., McGillicuddy et al., 2011) or through simple extrapolation from the empirical relationships shown in Figure 8.

4.7 Bloom geographic extent and intensity as determinants of subsequent cyst abundance

In a parallel series of analyses, we searched for a relationship between bloom geographic extent or intensity metrics and the abundance of cysts within various subregions or combinations of subregions later that same year (i.e., *blooms → cysts*). The only significant relationship between a geographic bloom metric and cyst abundance was between EGOM closure length and WGOM+EGOM 0-3 cm cysts (Fig. 11). This presumably reflects the upstream (EGOM) source of cells that lead to cysts deposited in that subregion and downstream (WGOM).

A significant relationship was also observed between bloom termination date and subsequent cyst abundance (Fig. 12A,B). Even stronger correlations were observed with cumulative shellfish toxicity per station and with bloom duration, both of which had highly significant regressions with the 0-3 cm cyst abundance (Figs. 13, 14). "Intensity" metrics like bloom duration and cumulative toxicity are therefore better reflections of cell concentrations than the coastline closure metrics which are based solely on whether the coastline received sufficient toxin exposure to justify closures and do not give a true indication of the concentration of toxic cells or the magnitude of shellfish toxicity.

There was no significant correlation between geographic or intensity bloom metrics and 0-1 cm cyst abundance, except for termination date and WGOM+EGOM cyst abundance (Fig. 12A). In contrast, several strong and significant relationships were apparent between these same metrics and 0-3 cm layer cyst abundance. Given the range in bloom termination dates and the rapid burial of many newly deposited cysts (Keafer et al., 1992), it is logical that the surface 0-1 cm layer would not contain all of the cysts from the preceding bloom. Instead, an inventory that includes 0-3 cm (or perhaps even deeper) would be a better representation of the cyst production from that year as long as the new deposition constitutes a significant

fraction of that inventory, which appears to be the case in the GOM given our significant regressions (Figs 13, 14).

It is tempting to consider the potential utility of the observed *blooms → cysts* relationships to estimate the inoculum size for the coming year, based on shellfish toxicity observations from the current year. This approach is complicated by the need to include cysts in the 0-3 cm layer for this relationship, whereas the germination inoculum probably derives from the top cm or so. Since the number of cysts in the surface 0-1 cm layer is 22.5-28.8% of the total in the top 3 cm for the three subregions over all survey years (Table 4), it is possible to calculate a probable surface layer percentage from the means of these subregional totals. Care must be taken with such an extrapolation, however, as several years (2004, 2007) stand out as outliers in this general relationship, particularly in the WGOM, as both years had nearly 50% of the cysts in the top cm. The year 2005 is an outlier in the opposite direction for the WGOM and EGOM, as surface-layer cysts were only 13.9 and 10.6% of the total cysts respectively.

5 Summary and Conclusions

Here we present a nine-year time series of cyst abundance surveys over large geographic scales in the GOM. These surveys delineate two major seedbeds, one in the BOF and one on the mid-coast Maine shelf. Cyst abundance varies by over an order of magnitude among years, and the area of the seedbeds varied 3-4 fold as well. Strong correlations were confirmed between the abundance of *A. fundyense* cysts in individual subregions or combinations of subregions and the geographic extent of the bloom the next year (*cysts → blooms*), as indicated by the length of coastline closed due to shellfish toxicity or the southernmost extent of closures. In contrast, with one exception, these geographic metrics did not correlate well with the number of cysts observed in the sediments in the fall following the blooms (*blooms → cysts*). Instead, there is a positive correlation between two bloom intensity metrics that are presumably more indicative of vegetative cell abundance (cumulative toxicity and duration) and the number of cysts the following fall. Nearly all of the significant relationships between blooms and subsequent cyst abundance are based on the 0-3 cm inventory, reflecting the need to account for cyst burial between the probable times of deposition (bloom termination) and the cyst surveys. For the *cysts → blooms* relationships, either the surface 0-1 cm or the 0-3 cm total cyst abundance can be used, although arguments can be made in favor of the use of the 0-1 cm surface layer for forecasts of future blooms.

From a management perspective, it is now possible to use the relationships of cyst abundance in the sediments to the geographic extent of blooms to estimate or forecast the extent of the forthcoming bloom's impact in the GOM based on an annual cyst survey. This empirical forecasting approach is simple in concept, does not require a numerical model, and is quite robust given the high statistical significance of the relationship when the year 2010 is excluded. A retrospective analysis of the accuracy of this approach compared to actual PSP closure data in the region is underway. Furthermore, the relationship between toxicity and cyst abundance could be used with bloom toxicity data to estimate the size of a bloom's cyst production. These results represent an important step towards understanding the

relationships between excystment and encystment in *A. fundyense* bloom dynamics in the GOM, and augment our predictive capability for this HAB-forming species.

Supplementary Material

Refer to Web version on PubMed Central for supplementary material.

Acknowledgments

References

Anderson, DM. Physiology and bloom dynamics of toxic *Alexandrium* species, with emphasis on life cycle transitions.. In: Anderson, DM.; Cembella, AD.; Hallegraeff, GM., editors. The Physiological Ecology of Harmful Algal Blooms. Springer-Verlag; Heidelberg: 1998. p. 29-48.

Anderson DM. The effects of temperature conditioning on the development and germination of *Gonyaulax tamarensis* (*Dinophyceae*) hypnozygotes. J. Phycol. 1980; 16:166–172.

Anderson DM, Aubrey DG, Tyler MA, Coats DW. Vertical and horizontal distributions of dinoflagellate cysts in sediments. Limnol. Oceanogr. 1982; 27(4):757–765.

Anderson DM, Chisholm SW, Watras CJ. The importance of life cycle events in the population dynamics of *Gonyaulax tamarensis*. Mar. Biol. 1983; 76:179–183.

Anderson DM, Couture DA, Kleindinst JL, Keafer BA, McGillicuddy DJ Jr. Martin JL, Richlen ML, Hickey JM, Solow AR. Understanding interannual, decadal level variability in paralytic shellfish poisoning toxicity in the Gulf of Maine: the HAB Index. Deep-Sea Res. II. this issue.

Anderson, DM.; Fukuyo, Y.; Matsuoka, K. Cyst methodologies.. In: Hallegraeff, GM.; Anderson, DM.; Cembella, AD., editors. Manual on Harmful Marine Microalgae, Monographs on Oceanographic Methodology. Vol. 11. UNESCO; 2003. p. 165-190.

Anderson DM, Keafer BA. An endogenous annual clock in the toxic marine dinoflagellate *Gonyaulax tamarensis*. Nature. 1987; 325:616–617. [PubMed: 3808064]

Anderson, DM.; Keafer, BA. Dinoflagellate cyst dynamics in coastal and estuarine waters.. In: Anderson, DM.; White, AW.; Baden, DG., editors. Toxic Dinoflagellates, Proc. 3rd Int'l Conf.; Elsevier, New York. 1985. p. 219-224.

Anderson DM, Keafer BA, Geyer WR, Signell RP, Loder TC. Toxic Alexandrium blooms in the western Gulf of Maine: the plume advection hypothesis revisited. Limnol. Oceanogr. 2005a; 50(1): 328–345.

Anderson DM, Keafer BA, McGillicuddy DJ, Mickelson MJ, Keay KE, Libby PS, Manning JP, Mayo CA, Whittaker DK, Hickey JM, He R, Lynch DR, Smith KW. Initial observations of the 2005 Alexandrium fundyense bloom in southern New England: General patterns and mechanisms. Deep-Sea Res. II. 2005b; 52(19-21):2856–2876.

Anderson DM, Kulis DM, Doucette GJ, Gallager JC, Balech E. Biogeography of toxic dinoflagellates in the genus Alexandrium from the northeast United States and Canada as determined by morphology, bioluminescence, toxin composition, and mating compatibility. Mar. Biol. 1994; 120:467–478.

Anderson DM, Lindquist NL. Time-course measurements of phosphorus depletion and cyst formation in the dinoflagellate *Gonyaulax tamarensis* Lebour. J. Exper. Mar. Biol. & Ecol. 1985; 86:1–13.

Anderson DM, Morel FMM. The seeding of two red tide blooms by the germination of benthic *Gonyaulax tamarensis* hypnocysts. Estuar. Coast. Mar. Sci. 1979; 8:279–293.

Anderson DM, Stock CA, Keafer BA, Bronzino Nelson A, Thompson B, McGillicuddy DJ, Keller M, Matrai PA, Martin J. *Alexandrium fundyense* cyst dynamics in the Gulf of Maine. Deep-Sea Res. II. 2005c; 52(19-21):2522–2542.

Anderson DM, Taylor CD, Armbrust EV. The effects of darkness and anaerobiosis on dinoflagellate cyst germination. Limnol. Oceanogr. 1987; 32:340–351.

Anderson DM, Townsend DW, McGillicuddy DJ, Turner JT. The Ecology and Oceanography of Toxic *Alexandrium fundyense* Blooms in the Gulf of Maine. Deep-Sea Res. II. 2005d; 52(19-21): 2365–2876.

Angeles S, Garces E, Rene A, Sampedro N. Life-cycle alternations in *Alexandrium minutum* natural populations from the NW Mediterranean Sea. Harmful Algae. 2012; 16:1–11.

Angeles S, Jordi A, Garces E, Basterretxea G, Palanques A. Alexandrium minutum resting cyst distribution dynamics in a confined site. Deep-Sea Res. II. 2010; 57(3–4):210–221.

Aretxabaleta AL, McGillicuddy DJ, Smith KW, Lynch DR. Model Simulations of the Bay of Fundy Gyre: 1. Climatological Results. J. Geophys. Res. 2008; 113 doi:10.1029/2007JC004480.

Aretxabaleta AL, McGillicuddy DJ, Smith KW, Manning JP, Lynch DR. Model simulations of the Bay of Fundy gyre: 2. Hindcasts for 2005-2007 reveal interannual variability in retentiveness. J. Geophys. Res. 2009; 114:C09005. doi:10.1029/2008JC004948.

Brooks DA, Townsend DW. Variability of the coastal current and nutrient pathways in the eastern Gulf of Maine. J. Mar. Res. 1989; 47:303–321.

Bravo I, Anderson DM. The effects of temperature, growth medium and darkness on excystment and growth of the toxic *dinoflagellate Gymnodinium catenatum* from northwest Spain. J. Plankton Res. 1994; 16:513–525.

Butman B, Aretxabaleta AL, Dickhudt PJ, Dalyander PS, Sherwood CR, Anderson DM, Keafer BA, Signell RP. Investigating the importance of sediment resuspension in *Alexandrium fundyense* cyst population dynamics in the Gulf of Maine. Deep-Sea Res. II. this issue.

Cho, HJ.; Matsuoka, K. Proceedings of 2nd International Workshop on Oceanography and Fisheries in the East China Sea. Nagasaki University; Japan: 1999. Dinoflagellate cyst composition and distribution in the surface sediments from the Yellow Sea and East China Sea. The East China Sea, 2.; p. 73-81.

Craib JS. A sampler for taking short undisturbed marine cores. J. Cons. Perm. Int. Explor. Mer. 1965; 30:34–39.

Crespo BG, Keafer BA, Ralston DK, Lind H, Farber D, Anderson DM. Dynamics of *Alexandrium fundyense* blooms and shellfish toxicity in the Nauset Marsh System of Cape Cod (Massachusetts, USA). Harmful Algae. 2011; 12:26–38.

Dale, B. Dinoflagellate resting cysts: 'benthic plankton'.. In: Fryxell, GA., editor. Survival Strategies of the Algae. Cambridge Univ. Press; Cambridge: 1983. p. 69-136.

Dale B. Marine dinoflagellate cysts as indicators of eutrophication and industrial pollution: A discussion. The Science of the Total Environment. 2000; 264:221–233.

Dale B. Marine dinoflagellate cysts as indicators of eutrophication and industrial pollution: a discussion. Science of the Total Environment. 2001; 264(3):235–240. [PubMed: 11213194]

Franks PJS, Anderson DM. Alongshore transport of a toxic phytoplankton bloom in a buoyancy current: *Alexandrium tamarensis* in the Gulf of Maine. Mar. Biol. 1992a; 112:153–164.

Franks PJS, Anderson DM. Toxic phytoplankton blooms in the southwestern Gulf of Maine: Testing hypotheses of physical control using historical data. Mar. Biol. 1992b; 112:165–174.

Genovesi B, Laabir M, Masseret E, Collos Y, Vaquer A, Grzebyk D. Dormancy and germination features in resting cysts of *Alexandrium tamarense* species complex (Dinophyceae) can facilitate

bloom formation in a shallow lagoon (Thau, southern France). J. Plankt. Res. 2009; 31(10):1209–1224.

Hattenrath TK, Anderson DM, Gobler CJ. The influence of anthropogenic nitrogen loading and meteorological conditions on the dynamics and toxicity of *Alexandrium fundyense* blooms in a New York (USA) estuary. Harmful Algae. 2010; 9:402–412.

He R, McGillicuddy DJ, Keafer BA, Anderson DM. Historic 2005 toxic bloom of *Alexandrium fundyense* in the western Gulf of Maine: 2. Coupled Biophysical Numerical Modeling. J. Geophys. Res.-Oceans. 2008; 113:C07040. doi:10.1029/2007JC004602.

Imai I, Itakura S, Itoh K. Life cycle strategies of the red tide causing flagellates *Chatonella* (Raphidophyceae) in the Seto Inland Sea. Mar. Poll. Bull. 1991; 23:165–170.

Keafer BA, Buesseler KO, Anderson DM. Burial of living dinoflagellate cysts in estuarine and nearshore sediments. Mar. Micropaleontol. 1992; 20:147–161.

Keafer BA, Churchill JH, Anderson DM. Blooms of the toxic dinoflagellate, *Alexandrium fundyense* in the Casco Bay region of the western Gulf of Maine: Advection from offshore source populations and interactions with the Kennebec River plume. Deep-Sea Res. II. 2005; 52(19-21):2631–2655.

Keafer, BA.; Churchill, JH.; Geyer, WR.; Signell, RP.; Hurst, JW.; Bean, LL.; Pettigrew, NR.; Anderson, DM. Detection of *Alexandrium fundyense* bloom initiation and transport in the western Gulf of Maine, USA, using mussel bags (*Mytilus edulis*) on offshore hydrographic moorings.. In: Steidinger, KA.; Landsberg, JH.; Tomas, CR.; Vargo, GA., editors. Harmful Algae 2002. Florida Fish and Wildlife Conservation Commission. Florida Institute of Oceanography, and Intergovernmental Oceanographic Commission of UNESCO; St. Petersburg, Florida, USA.: 2004. p. 285-287.

Kirn SL, Townsend DW, Pettigrew NR. Suspended *Alexandrium* spp. hypnozygotes cysts in the Gulf of Maine. Deep-Sea Res. II. 2005; 52(19-21):2543–2559.

Kleindinst JL, Anderson DM, McGillicuddy DJ Jr. Stumpf RP, Fisher KM, Darcie Couture D, Hickey JM, Nash C. Categorizing the severity of paralytic shellfish poisoning outbreaks in the Gulf of Maine for forecasting and management. Deep-Sea Res. II. this issue.

Kremp A, Anderson DM. Factors regulating germination of resting cysts of the spring bloom dinoflagellate *Scrippsiella hangoei* from the northern Baltic Sea. Journal of Plankton Research. 2000; 22(7):1311–1327.

Lee, JB.; Matsuoka, K. Distribution of dinoflagellate cyst from surface sediments in southern Korean waters.. Proceedings of 2nd International Symposium on the Marine Science Exploitation of Marine Resources; Korea. Cheju National University; 1994. p. 1-20.

Li Y, He R, McGillicuddy DJ. Seasonal and interannual variability in Gulf of Maine hydrodynamics: 2002-2011. Deep-Sea Res. II. this issue.

Li Y, He R, McGillicuddy DJ Jr. Anderson DM, Keafer BA. Investigation of the 2006 Alexandrium fundyense bloom in the Gulf of Maine: In situ observations and numerical modeling. Cont. Shelf Res. 2009; 29(17):2069–2082.

Lilly EL, Halaynch KM, Anderson DM. Species boundaries and global biogeography of the Alexandrium tamarense complex (Dinophyceae). J. Phycol. 2007; 43:1329–1338.

Lynch DR, Holboke MJ, Naimie CE. The Maine coastal current: spring climatological circulation. Cont. Shelf Res. 1997; 17:605–634.

Martin JL, LeGresley MM, Hanke A. Thirty years - Alexandrium fundyense cyst, bloom dynamics and shellfish toxicity in in the Bay of Fundy, eastern Canada. Deep-Sea Res. II. this issue.

Martin, JL.; LeGresley, MM.; Hanke, A.; Page, FH. *Alexandrium fundyense* - red tides, PSP shellfish toxicity, salmon mortalities and human illnesses in 2003-04 – before and after.. Proceedings of the 12th International Conference on Harmful Algae.; Copenhagen. 2008; International Society for the Study of Harmful Algae and Intergovernmental Oceanographic Commission of UNESCO; 2008. p. 206-208.

Martin JL, White AW. Distribution and abundance of the toxic dinoflagellate *Gonyaulax excavata* in the Bay of Fundy. Can. J. Fish. Aquat. Sci. 1988; 45:1968–1975.

Matrai P, Thompson B, Keller M. Circannual excystment of resting cysts of *Alexandrium* spp. from eastern Gulf of Maine populations. Deep-Sea Res. II. 2005; 52:2560–2568.

Matsuoka, K.; Fukuyo, Y. Technical Guide for Modern Dinoflagellate Cyst Study. WESTPAC-HAB/WESTPAC/IOC; Tokyo: 2000.

McGillicuddy DJ Jr. Anderson DM, Lynch DR, Townsend DW. Mechanisms regulating large-scale seasonal fluctuations in *Alexandrium fundyense* populations in the Gulf of Maine: Results from a physical-biological model. Deep-Sea Res. II. 2005; 52(19-21):2698–2714.

McGillicuddy DJ Jr. Brosnahan ML, Couture DA, He R, Keafer BA, Manning JP, Pilskaln C, Townsend DW, Anderson DM. A red tide of *Alexandrium fundyense* in the Gulf of Maine. Deep-Sea Res. II. this issue-a.

McGillicuddy DJ Jr. Signell RP, Stock CA, Keafer BA, Keller MD, Hetland RD, Anderson DM. A mechanism for offshore initiation of harmful algal blooms in the coastal Gulf of Maine. J. Plankt. Res. 2003; 25(9):1131–1138.

McGillicuddy DJ Jr. Townsend DW, He R, Keafer BA, Kleindinst JL, Li Y, Manning JP, Mountain DG, Thomas MA, Anderson DM. Suppression of the 2010 *Alexandrium fundyense* bloom by changes in physical, biological, and chemical properties of the Gulf of Maine. Limnol. Oceanogr. 2011; 56(6):2411–2426.

McGillicuddy DJ Jr. D.W. Townsend DW, Keafer BA, Thomas MA, Anderson DM. Georges Bank: a leaky incubator of *Alexandrium fundyense* blooms. Deep-Sea Res. II. this issue-b.

Miyazono A, Nagai S, Kudo I, Tanizawa K. Viability of *Alexandrium tamarense* cysts in the sediment of Funka Bay, Hokkaido, Japan: Over a hundred year survival times for cysts. Harmful Algae. 2012; 16:81–88. DOI: 10.1016/j.hal.2012.02.001.

Ní Rathaille A, Raine R. Seasonality in the excystment of *Alexandrium minutum* and *Alexandrium tamarense* in Irish coastal waters. Harmful Algae. 2011; 10:629–635.

Pettigrew NR, Churchill JH, Janzen CD, Mangum LJ, Signell RP, Thomas AC, Townsend DW, Wallinga JP, Xue H. The kinematic and hydrographic structure of the Gulf of Maine Coastal Current. Deep-Sea Res. II. 2005; 52(19-21):2369–2391.

Pfiester, LA.; Anderson, DM. Dinoflagellate reproduction.. In: Taylor, FJR., editor. The Biology of Dinoflagellates. Blackwell Scientific Publications, Ltd.; 1987. p. 611-648.

Pilskaln CH, Anderson DM, McGillicuddy DJ Jr. Keafer BA, Hayashi K, Norton K. Spatial and temporal variability of *Alexandrium* cyst fluxes in the Gulf of Maine: Relationship to seasonal particle export and resuspension. Deep-Sea Res. II. this issue-a.

Pilskaln CH, Hayashi K, Keafer BA, Anderson DM, McGillicuddy DJ. Benthic nepheloid layers in the Gulf of Maine and *Alexandrium* cyst inventories. Deep-Sea Res. II. this issue-b.

Rengefors K, Anderson DM. Environmental and endogenous regulation of cyst germination in two freshwater dinoflagellates. J. Phycol. 1998; 34(4):568–577.

Ribeiro S, Berge T, Lundholm N, Andersen TJ, Abrantes F, Ellegaard M. Phytoplankton growth after a century of dormancy illuminates past resilience to catastrophic darkness. Nat. Comm. 2011; 2:311. DOI: 10.1038/ncomms1314.

Shull D, Kremp A, Mayer LM. Bioturbation, germination and deposition of *Alexandrium fundyense* cysts in the Gulf of Maine. Deep-Sea Res. II. this issue.

Stock CA, McGillicuddy DJ, Solow AR, Anderson DM. Evaluating hypotheses for the initiation and development of *Alexandrium fundyense* blooms in the western Gulf of Maine using a coupled physical-biological model. Deep-Sea Res. II. 2005; 52(19-21):2715–2744.

Townsend DW, Pettigrew NR, Thomas AC. Offshore blooms of the red tide dinoflagellate, *Alexandrium* sp., in the Gulf of Maine. Cont. Shelf Res. 2001; 21:347–369.

Turgeon, J.; Cembella, AD.; Therriault, J-C.; Béland, P. Spatial distribution of resting cysts of Alexandrium spp. in sediments of the lower St. Lawrence Estuary and the Gaspé coast (eastern Canada).. In: Granéli, E., editor. Toxic Marine Phytoplankton. Elsevier; New York: 1990. p. 238-243.

Turpin DH, Dobel PER, Taylor FJR. Sexuality and cyst formation in Pacific strains of the toxic dinoflagellate *Gonyaulax tamarensis*. J. Phycol. 1978; 14:235–238.

Tyler MA, Coats DW, Anderson DM. Encystment in a dynamic environment: deposition of dinoflagellate cysts by a frontal convergence. Mar. Ecol. Prog. Ser. 1982; 7:163–178.

Wall D. Biological problems concerning fossilizable dinoflagellates. Geoscience and Man. 1971; III:1–15.

Yamaguchi M, Itakura S, Imai I, Ishida Y. A rapid and precise technique for enumeration of resting cysts of *Alexandrium* spp. (Dinophyceae) in natural sediments. Phycologia. 1995; 34:207–214.
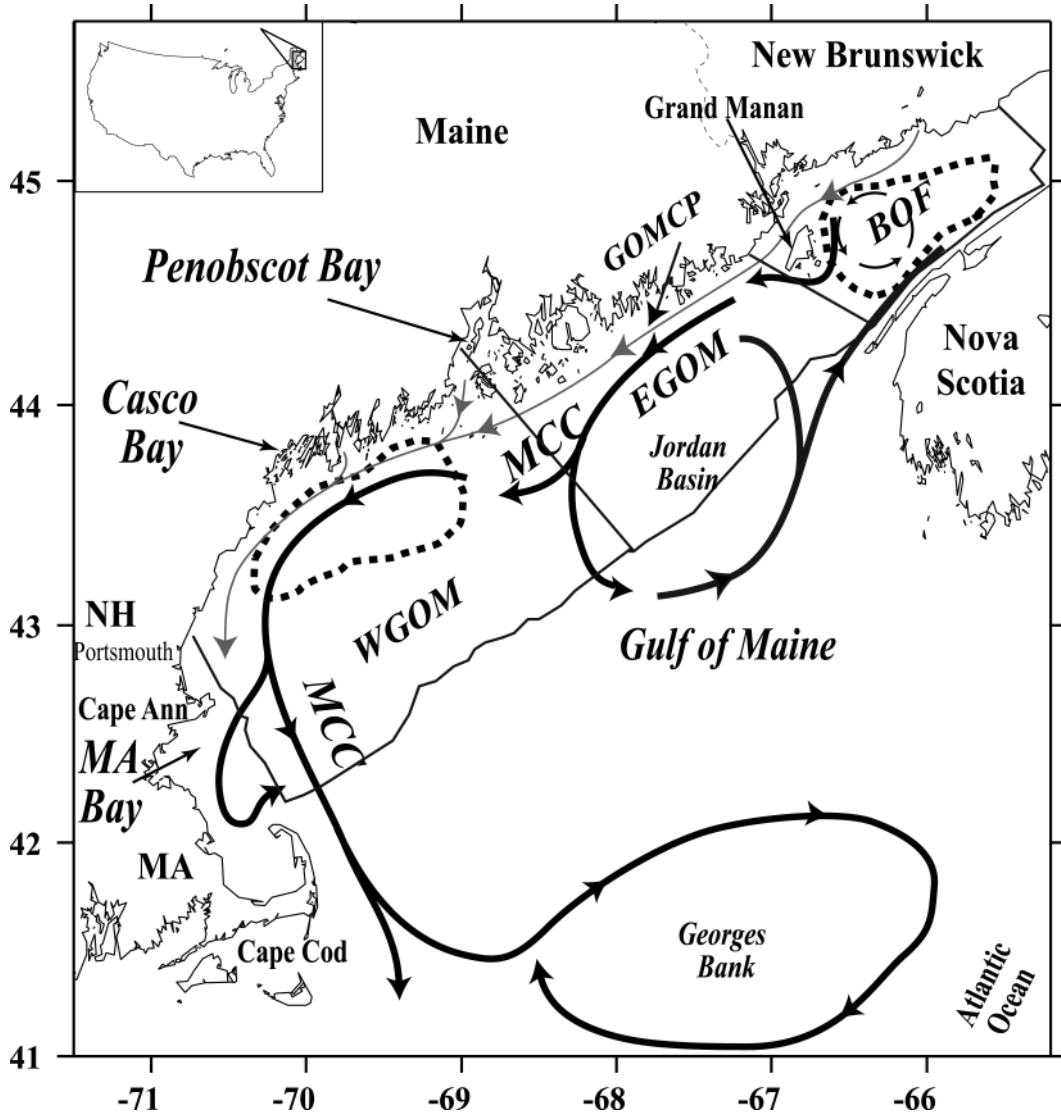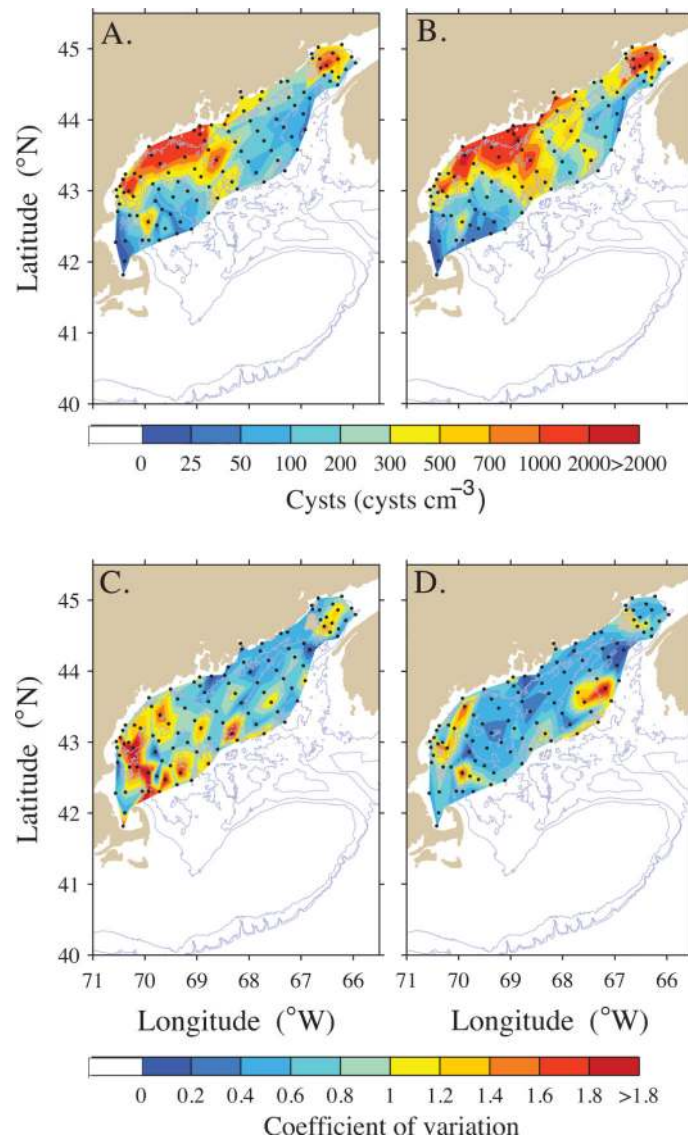
Figure 1.
Designation of the eastern Gulf of Maine (EGOM), western Gulf of Maine (WGOM), and Bay of Fundy (BOF) subregions of the study area. Note that the outer boundaries of these regions are defined by the cyst mapping survey areas. General locations of the cyst mid-coast Maine seedbed and the BOF seedbed are indicated by dotted lines. Portions of the WGOM (e.g., Massachusetts Bay) are not included in this definition, but are indeed part of the GOM. Likewise, the BOF subregion does not include the entire bay. Major current systems are shown (black = Maine Coastal Current (MCC); light grey = Gulf of Maine Coastal Plume (GOMCP; Keafer et al., 2005). (NH - New Hampshire; MA – Massachusetts)
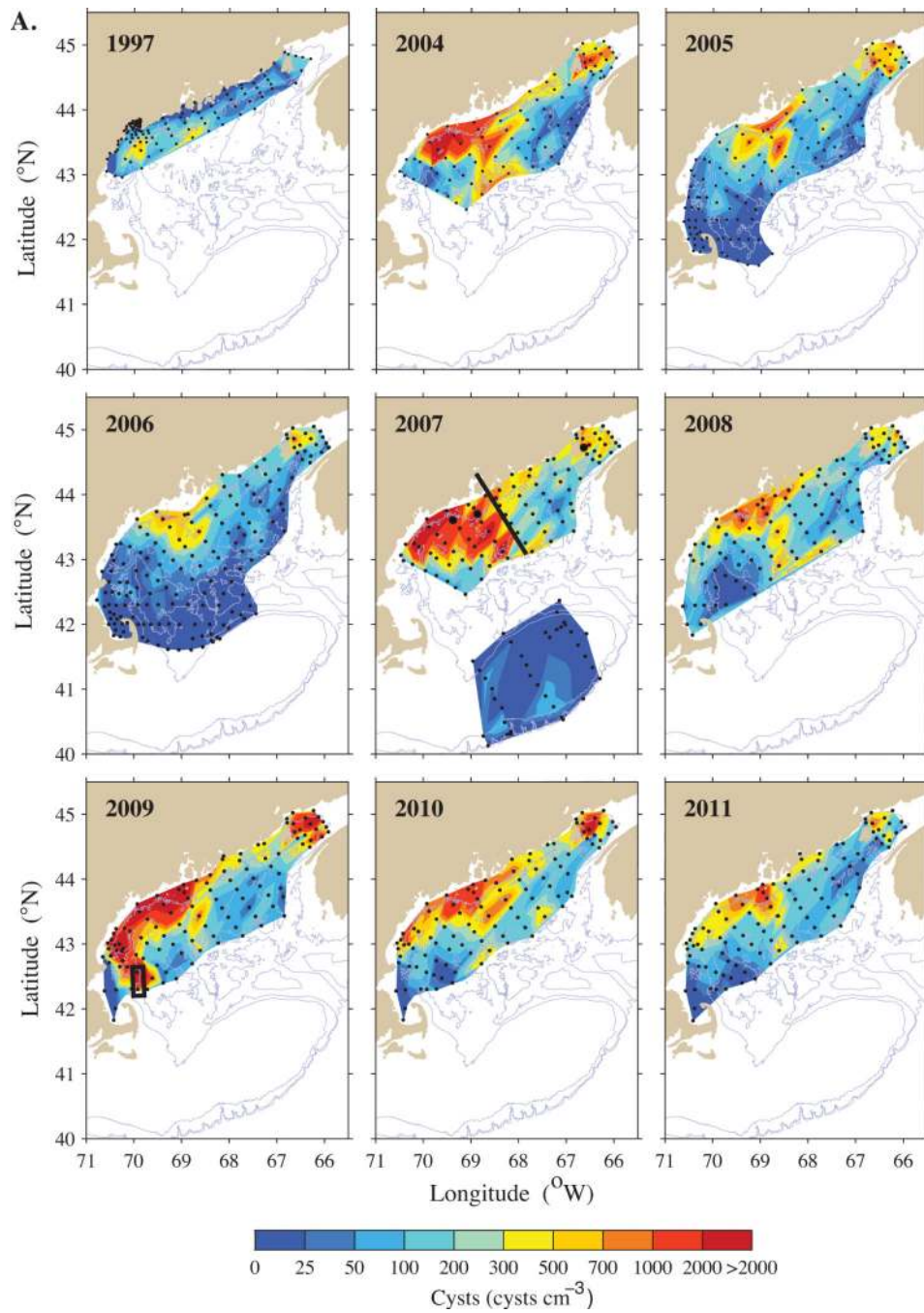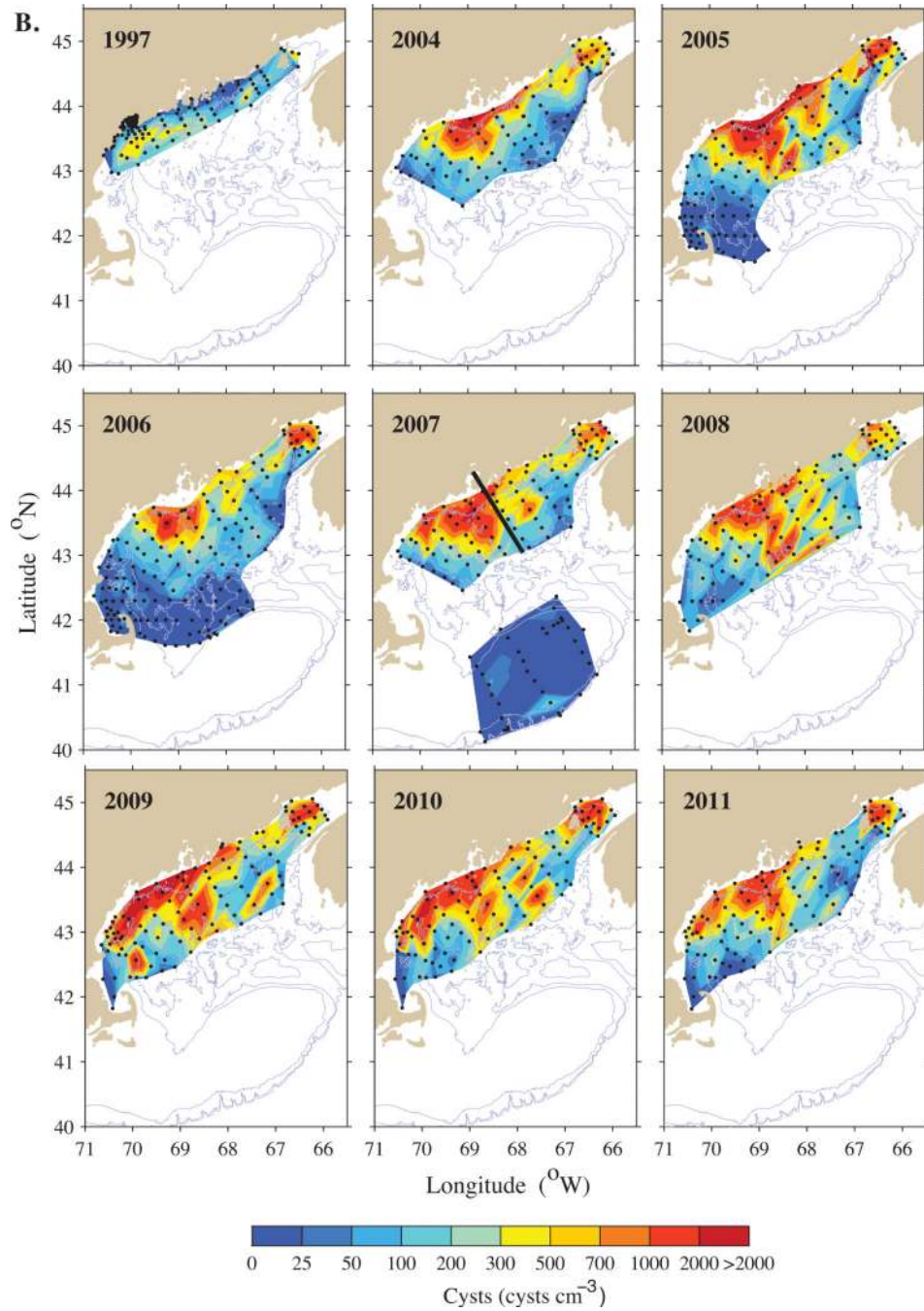
Figure 2.

Large-scale maps of *A. fundyense* cyst abundance (cysts cm^{-3}) in the Gulf of Maine for each of the survey years. (A) top 0-1 cm layer of sediments; (B) the 1-3 cm layer. Station locations are indicated by black dots. The three larger dots in the 2007 map show location of stations analyzed in Figure 5. The two stations enclosed in the box in the 2009 map shows locations of stations analyzed in Figure 7. The black line in 2007 separates the WGOM and EGOM subregions.

Figure 3.
Multi-year (2004 – 2011) arithmetic mean cyst abundance (cysts cm^{-3}) and coefficient of variation, CV. (A) surface (0-1 cm) sediment layer mean cyst abundance; (B) 1-3 cm layer mean cyst abundance; (C) CV of surface layer cyst abundance; and (D) CV of 1-3 cm layer cyst abundance.
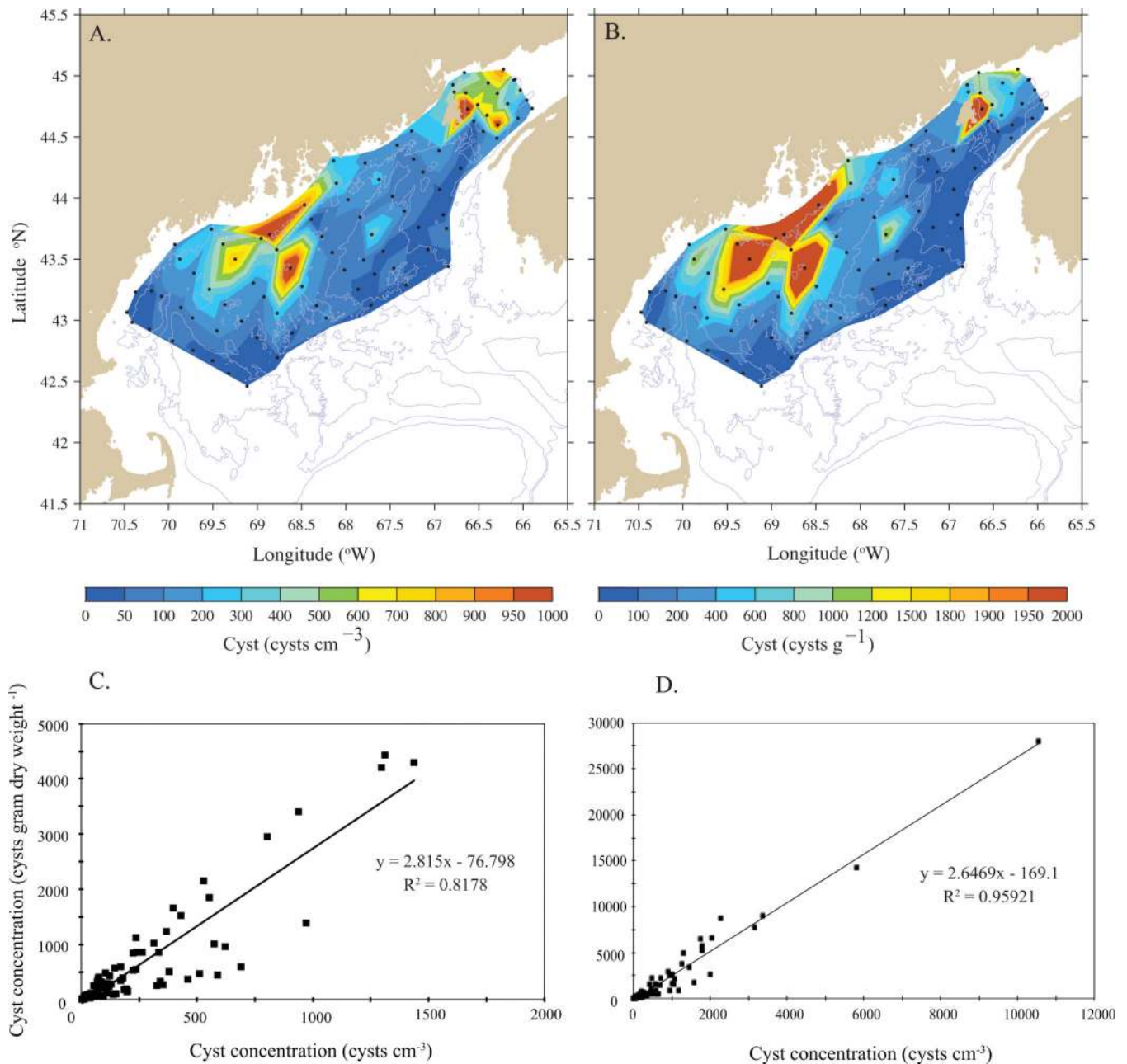
Figure 4.
Comparison of volumetric and mass measures of cyst abundance for the subset of stations in 2005 for which both assays are available. (A) areal contour map of cysts cm^{-3}; (B) contour map of cysts g^{-1} dry weight, DW; (C) first-order regression of cysts cm^{-3} versus cysts g^{-1} DW (0-1 cm). (D) first-order regression of cysts cm^{-3} versus cysts g^{-1} DW (1-3 cm layer). The regressions in C and D are highly significant (p < 0.0001).
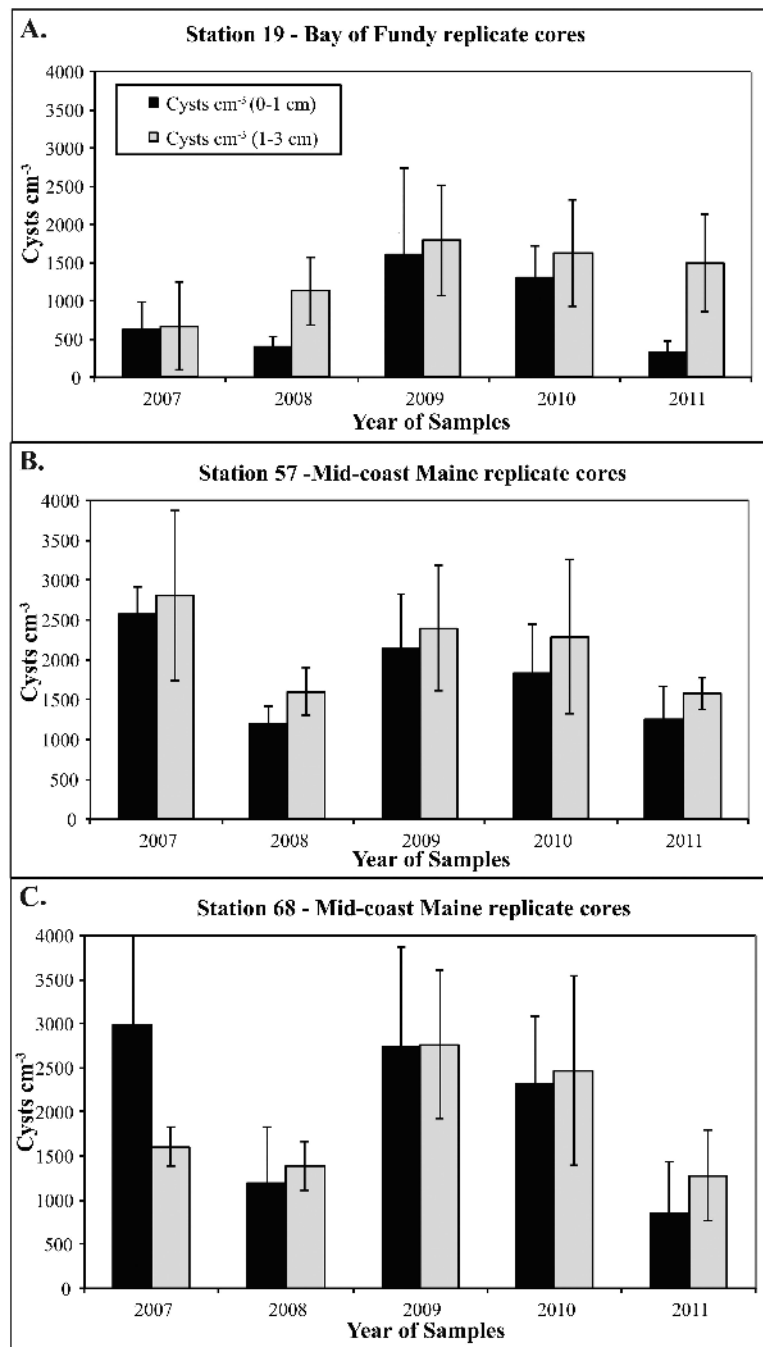
Figure 5.
Histogram plots of stations where six replicate cores were taken during the 2007-2011 cyst surveys. (A) BOF seedbed station (19); (B) Mid-coast Maine seedbed station (57); C) Mid-coast Maine seedbed station (68). These stations are noted with large dots in Figure 2, year 2007.
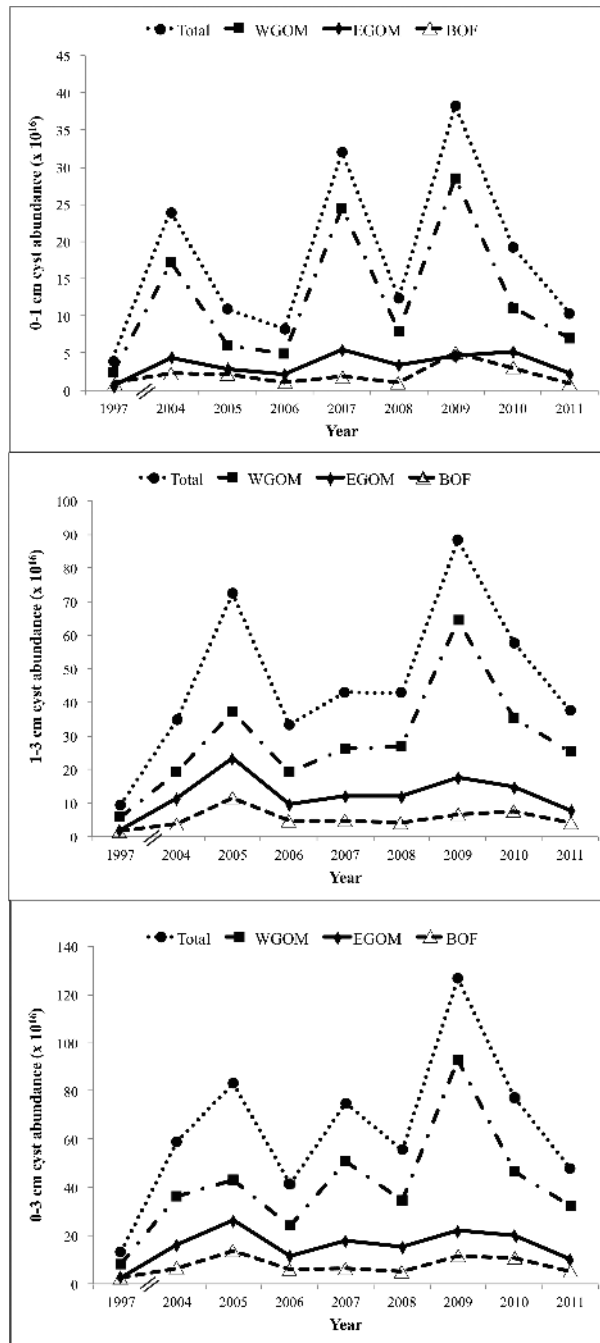
Figure 6.
Line plots showing cyst abundance (cysts $\times$ 10^{16}) in the WGOM, EGOM and BOF
subregions through time. (A) surface (0-1 cm); (B) deep (1-3 cm); (C) total (0-3 cm).

A.

B.
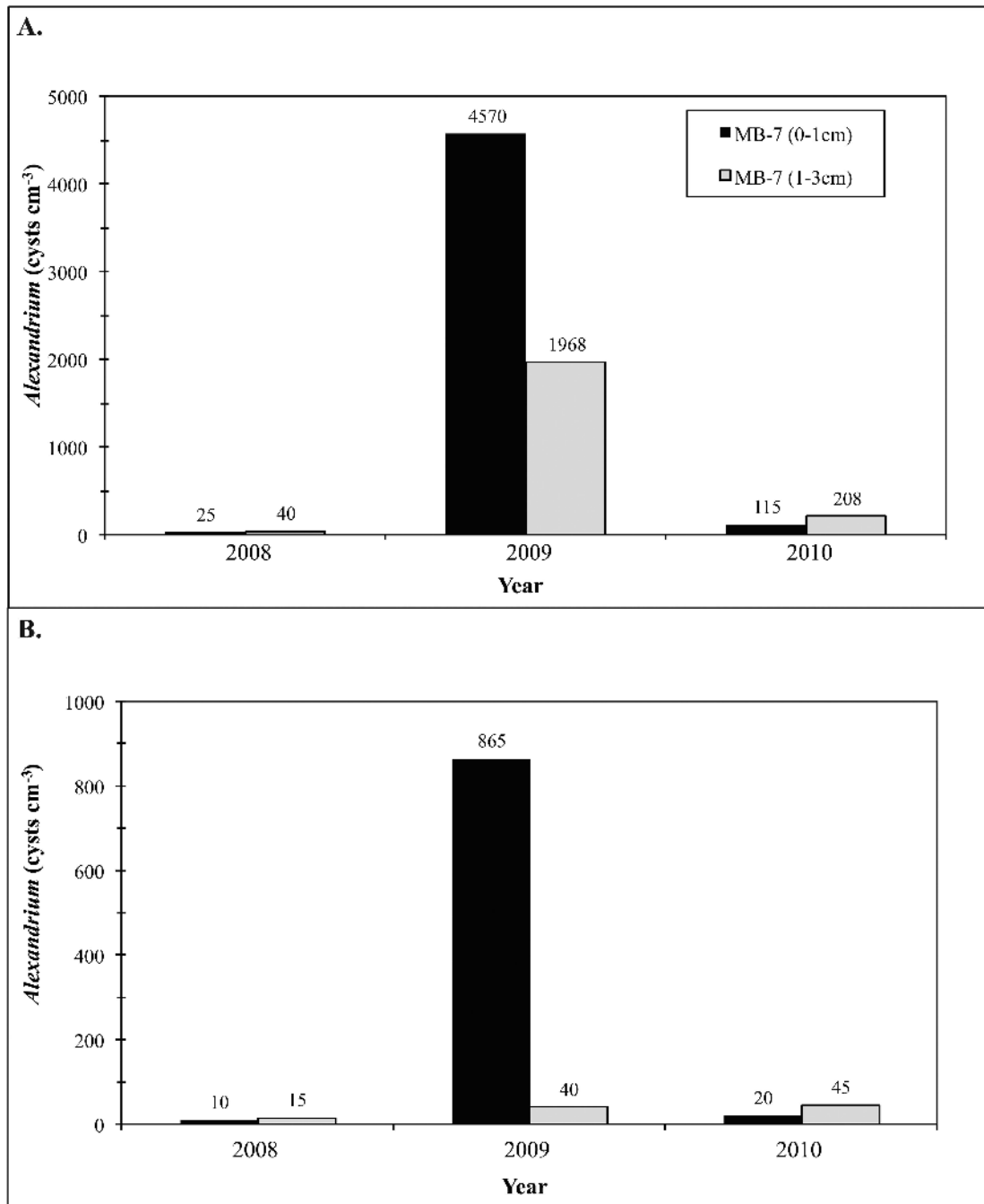
Figure 7.
Time series of cyst abundance at two stations located within the area of the 2009 mid-coast Maine seedbed expansion (stations MB-7 and MB-12; locations are shown in enclosed rectangle in Figure 2, year 2009).
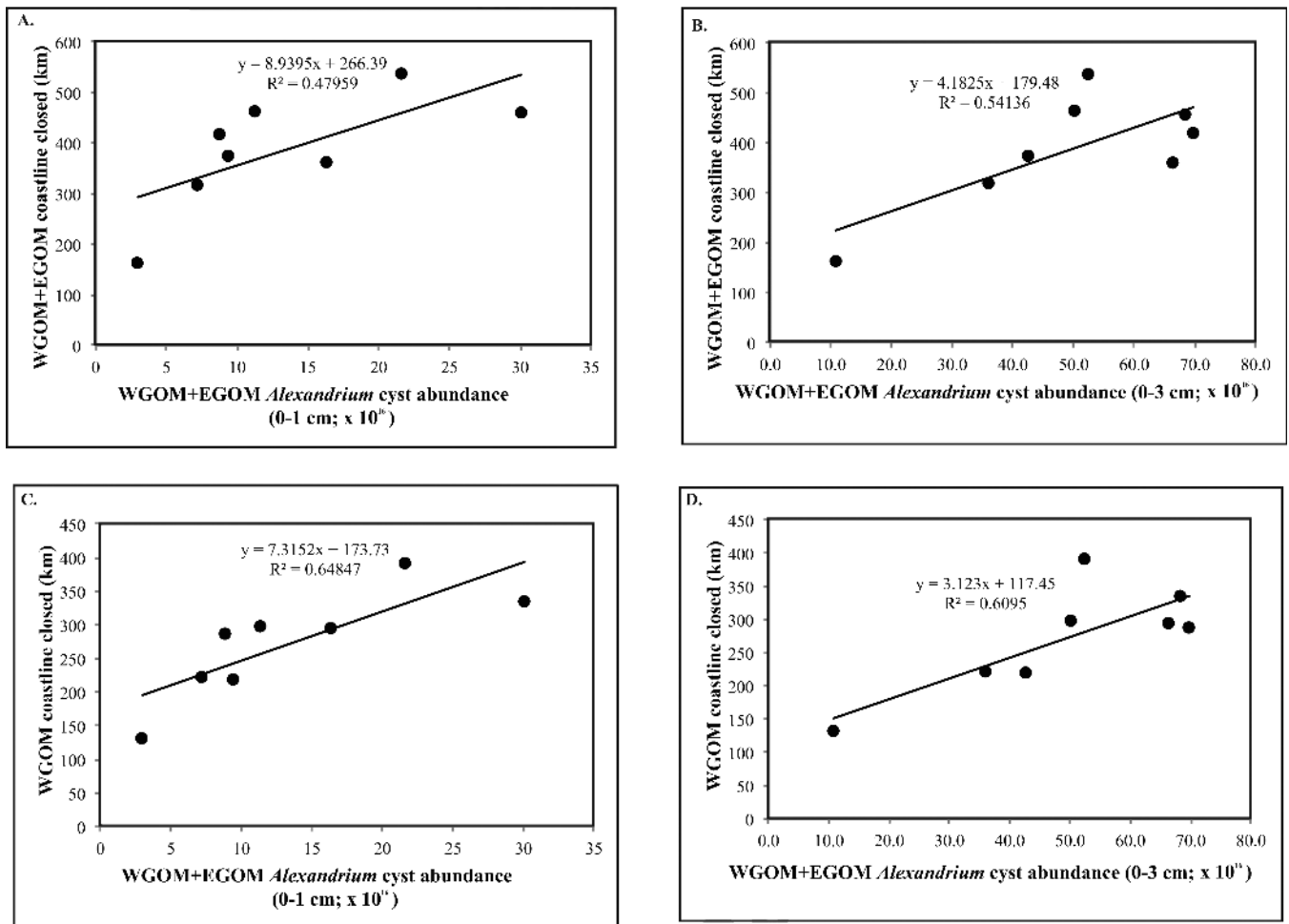
Figure 8.
Cyst abundance versus geographic extent of toxicity the following year. (A) WGOM
+EGOM cysts (0-1 cm) versus WGOM+EGOM coastline closed. The relationship is not
significant (p=0.0568) (B) WGOM+EGOM cysts (0-3 cm) versus WGOM+EGOM coastline
closed. The relationship is significant (p = 0.0374); (C) WGOM+EGOM cysts (0-1 cm)
versus WGOM coastline closed. The relationship is significant (p = 0.0016). (D) WGOM
+EGOM cysts (0-3 cm) versus WGOM coastline closed. The relationship is significant (p =
0.0222).
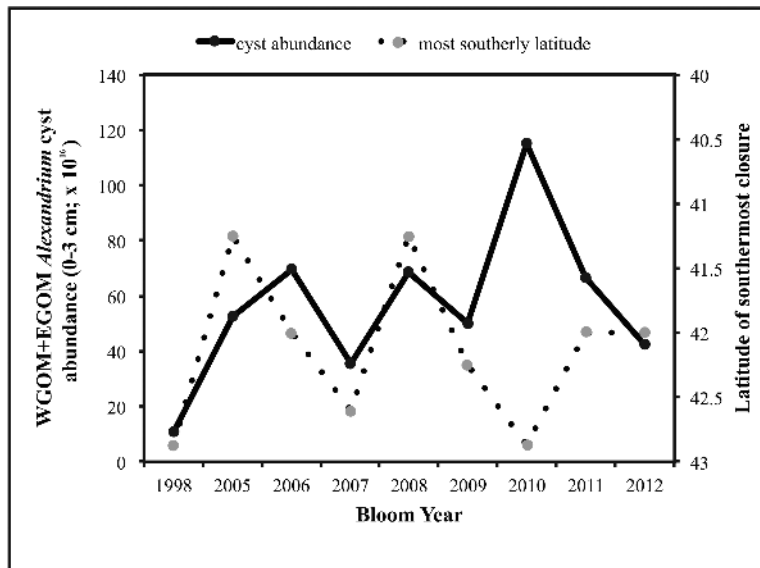
Figure 9.
Time-series of cyst abundance (cysts $\times 10^{16}$) in the western Gulf of Maine (WGOM) and the latitude of southernmost closure the following year (note axis reversal).
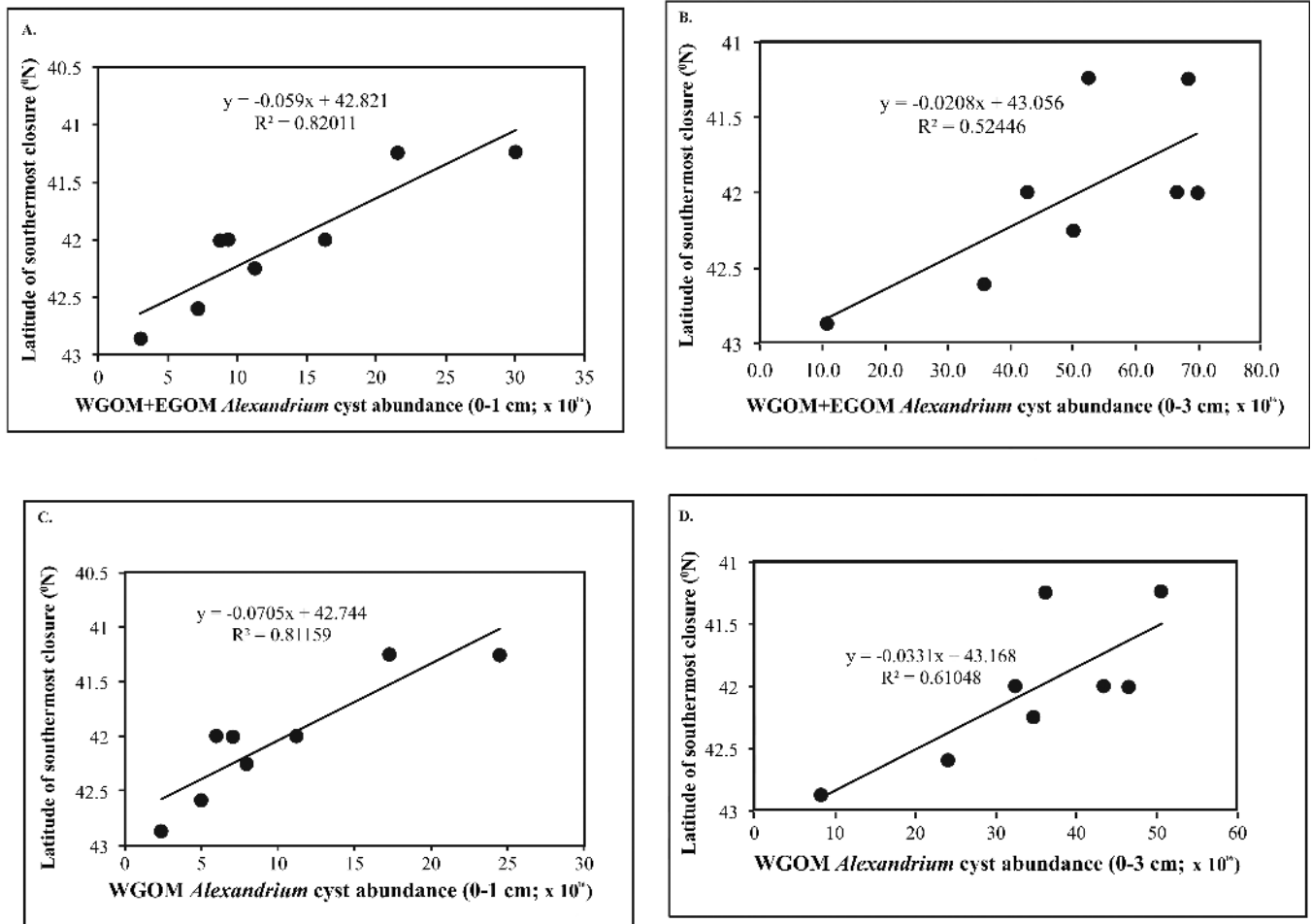
Figure 10.

Relationship between cyst abundance (cysts $\times 10^{16}$) and latitude of the southernmost shellfish harvesting closure due to PSP toxins the following year. (A) WGOM+EGOM cyst abundance (0-1 cm). The relationship is significant (p=0.0020); (B) WGOM+EGOM cyst abundance (0-3 cm). The relationship is significant (p=0.0042); (C) WGOM cyst abundance (0-1 cm). The relationship is significant (p=0.0023); (D) WGOM cyst abundance (0-3 cm). The relationship is significant (p = 0.0042).
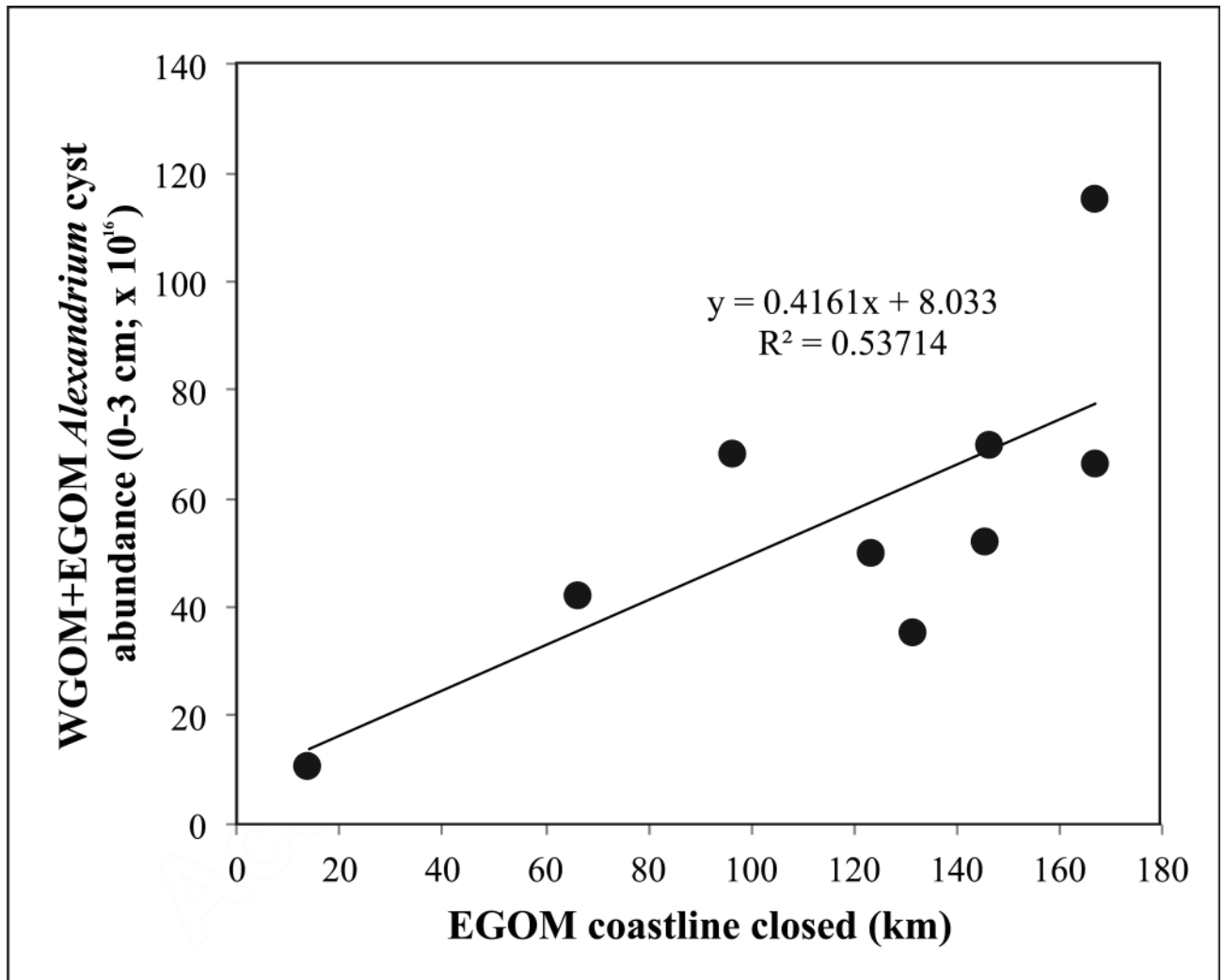
Figure 11.
Relationship between EGOM coastline closed (km) and WGOM+EGOM total (0-3 cm) cyst abundance later that same year. The relationship is significant (p = 0.0246).
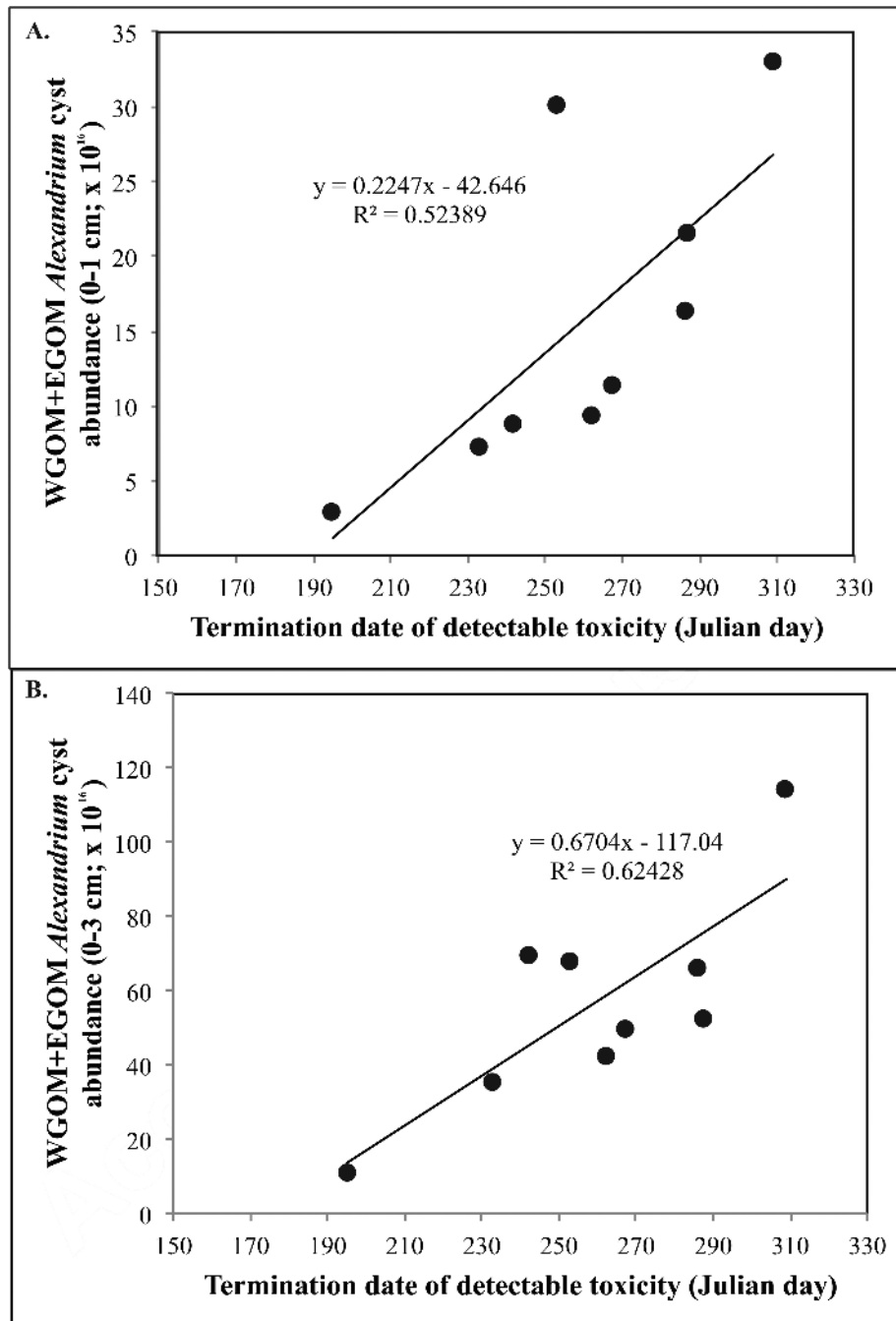
Figure 12.
Relationship between termination date of toxicity and (A) WGOM+EGOM cyst abundance (0-1 cm) later that same year. The relationship is significant (p = 0.0277). (B) WGOM +EGOM cyst abundance (0-3 cm) later that same year. The relationship is significant (p = 0.0112).
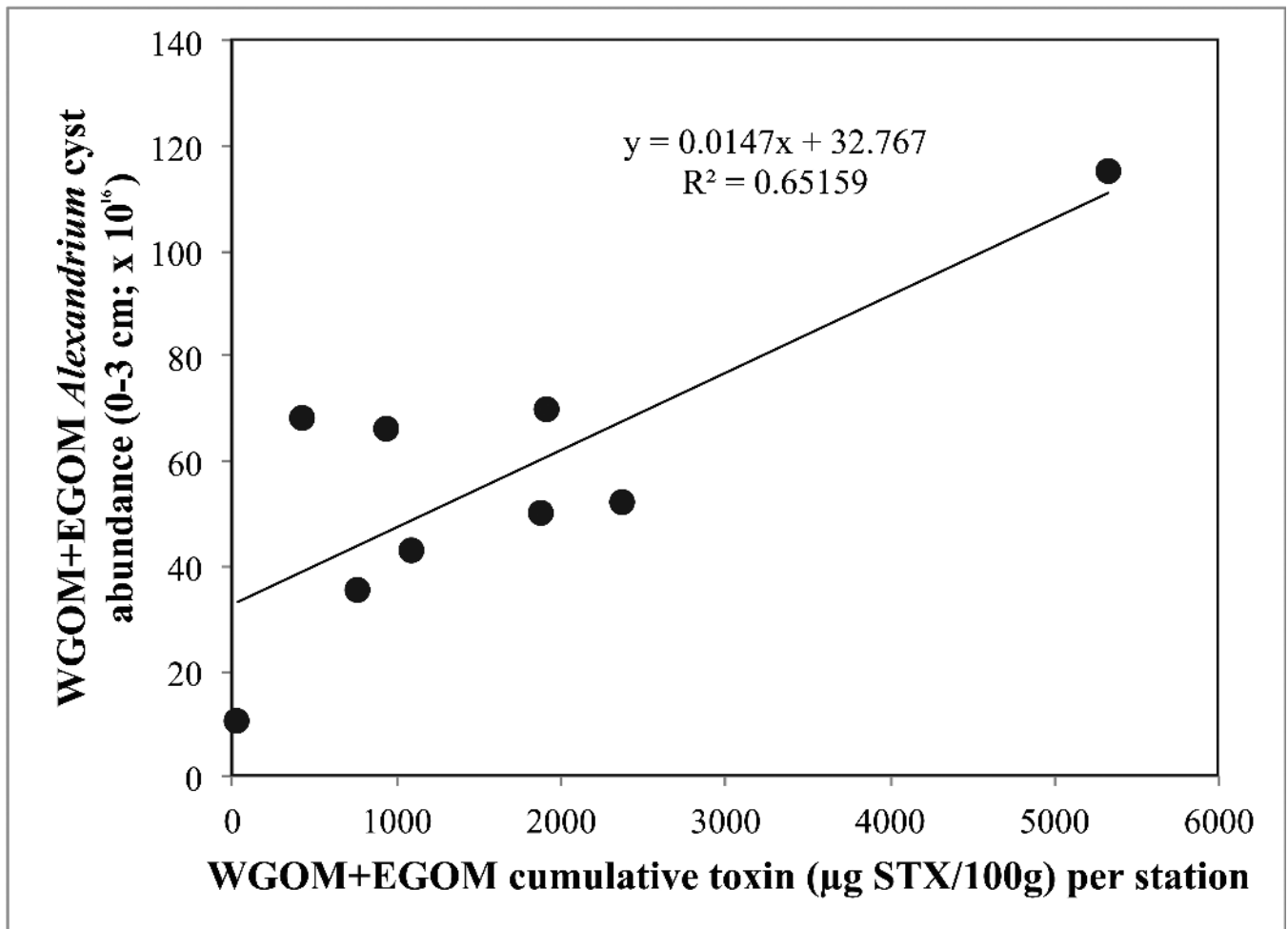
Figure 13.
Relationship between WGOM+EGOM cumulative shellfish toxicity (µg STX 100g^{-1}) per station and WGOM+EGOM cyst abundance (0-3 cm) later that same year. The relationship is significant (p = 0.0085).
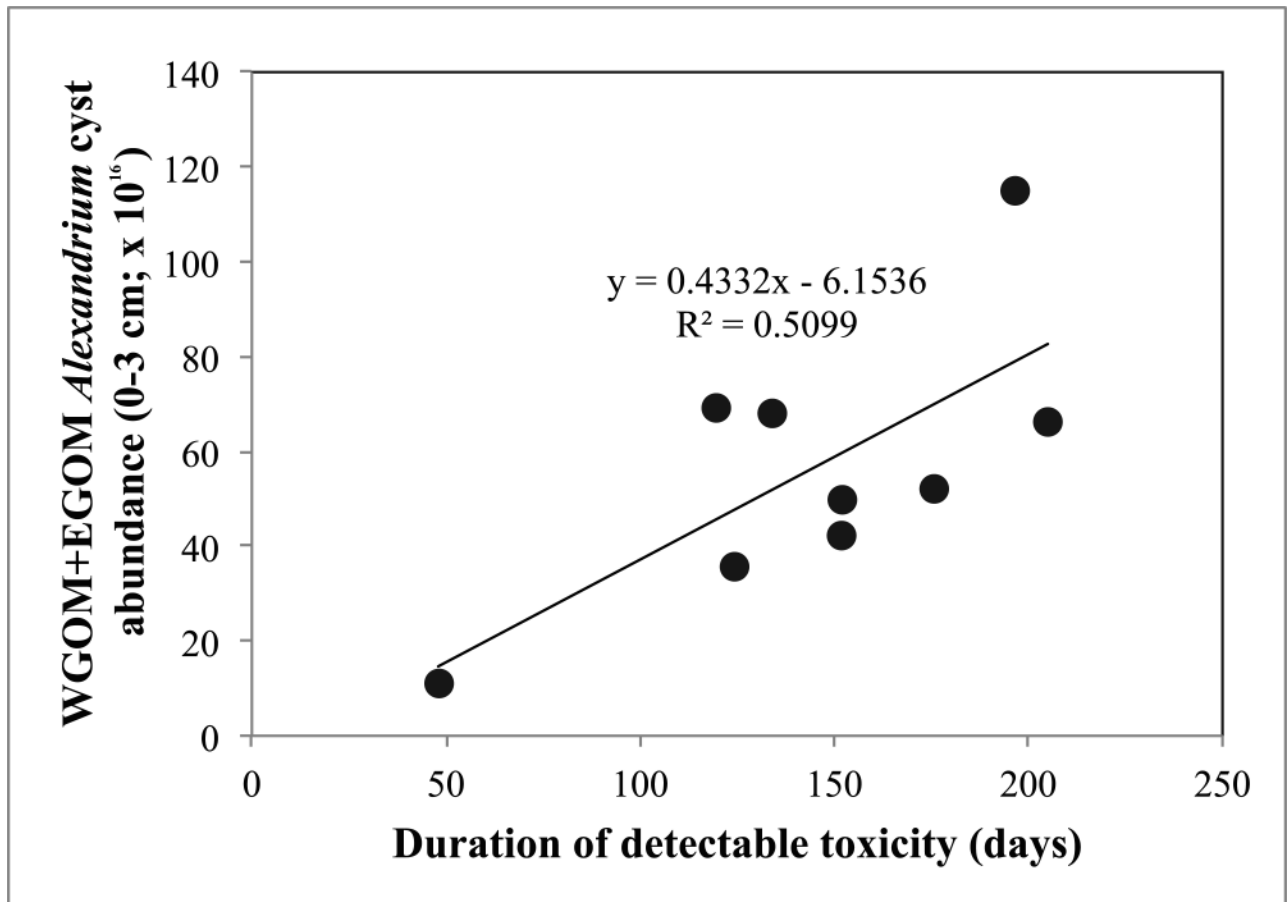
Figure 14.
Relationship between duration of detectable shellfish toxicity in the WGOM+EGOM and WGOM+EGOM cyst abundance (cysts $\times 10^{16}$) (0-3 cm) later that same year. The relationship is significant (p = 0.0084).

Table 1

Areas of GOM cyst seedbeds (km^2). Seedbeds defined as the area within the > 300 cysts cm^{-3} contour.

Year	WGOM	BOF	Total
2004	15,634	2,241	17,874
2005	6,674	2,605	9,279
2006	5,634	1,187	6,820
2007	19,393	3,164	22,557
2008	9,543	1,507	11,050
2009	17,308	4,383	21,691
2010	16,225	2,142	18,366
2011	8,885	1,108	9,993
Mean	**12,412**	**2,292**	**14,704**
SD	**5,307**	**1,102**	**6,107**

Table 2

Cyst abundance in GOM subregions, 1997, 2004-2011. Comparisons are given between each of these years and the mean cyst abundance for each subregion for 2004-2011 [*] (expressed as the % change relative to the mean cyst abundance for that subregion and layer). All cyst abundance values given as 10^{16} cysts.

0-1 cm

	WGOM cysts	% change WGOM	EGOM cysts	% change EGOM	WGOM +EGOM cysts	% change WGOM +EGOM	BOF cysts	% change BOF	total WGOM+ EGOM+ BOF cysts	% change total
1997	2.4	17	0.6	17	3.0	17	1.0	52	4.0	20
2004	17.2	119	4.4	122	21.6	120	2.3	119	23.9	120
2005	6.0	42	2.8	79	8.8	49	2.1	109	10.9	55
2006	5.0	35	2.2	61	7.2	40	1.1	58	8.3	42
2007	24.5	170	5.6	156	30.1	167	1.9	98	32.0	160
2008	7.9	55	3.4	94	11.3	63	1.1	58	12.4	62
2009	28.5	198	4.6	129	33.1	184	5.1	262	38.2	192
2010	11.2	77	5.1	144	16.3	91	3.0	153	19.3	97
2011	7.0	49	2.3	65	9.4	52	0.9	48	10.3	52
Mean	**14.4**	**100**	**3.6**	**100**	**18.0**	**100**	**1.9**	**100**	**19.9**	**100**

1-3 cm [**]

	WGOM cysts	% change WGOM	EGOM cysts	% change EGOM	WGOM+EGOM	% change WGOM+EGOM	BOF	% change BOF	total	% change total
1997	5.8	17	2.0	16	7.8	17	1.6	28	9.4	18
2004	19.1	57	11.7	93	30.8	66	4.0	70	34.8	67
2005	37.3	110	23.6	188	60.9	131	11.4	199	72.3	139
2006	19.1	56	9.6	76	28.6	62	4.7	82	33.3	64
2007	26.1	77	12.2	97	38.3	83	4.7	82	43.0	82
2008	26.7	79	12.1	96	38.8	84	4.0	71	42.9	82
2009	64.4	190	17.5	139	81.9	177	6.5	113	88.4	170
2010	35.3	104	14.9	118	50.1	108	7.6	133	57.8	111
2011	25.3	75	8.0	63	33.3	72	4.2	72	37.5	72
Mean	**33.8**	**100**	**12.6**	**100**	**46.4**	**100**	**5.7**	**100**	**52.1**	**100**

				0-3 cm						
1997	8.3	17	2.5	15	10.8	17	2.6	34	13.4	19
2004	36.3	75	16.0	99	52.4	81	6.3	82	58.7	81
2005	43.3	90	26.4	164	69.7	108	13.5	176	83.2	115
2006	24.1	50	11.7	73	35.8	56	5.8	76	41.6	58
2007	50.6	105	17.8	110	68.3	106	6.6	86	75.0	104
2008	34.6	72	15.5	96	50.1	78	5.2	67	55.3	77
2009	92.9	193	22.1	137	115.0	179	11.5	151	126.6	176
2010	46.5	96	20.0	124	66.5	103	10.6	138	77.1	107
2011	32.3	67	10.3	64	42.6	66	5.2	68	47.8	66
Mean	**48.2**	**100**	**16.2**	**100**	**64.4**	**100**	**7.7**	**100**	**72.1**	**100**

The mean area occupied by the cyst survey = 2.79×10^{14} cm^2 for the WGOM, 1.86×10^{14} cm^2 for the EGOM and 0.43×10^{14} cm^2 for the BOF.

[*] 1997 is not included in the calculated mean because the sampling domain was significantly smaller than the other years.

[**] Note: values for 1-3cm abundance have been multiplied by 2 to yield the total cysts in a 2 cm thick layer

Table 3

Cyst abundances ($\times 10^{16}$) and percentages of total (shaded in grey) by subregion.

YEAR	Surface (0-1 cm)							1-3 cm							Total (0-3 cm)						
	WGOM cysts	% of total	EGOM cysts	% of total	BOF cysts	% of total	TOT cysts	WGOM cysts	% of total	EGOM cysts	% of total	BOF cysts	% of total	TOT cysts	WGOM cysts	% of total	EGOM cysts	% of total	BOF cysts	% of total	TOT cysts
1997	2.4	60.0	0.6	15.0	1.0	25.0	4.0	5.8	61.7	2.0	21.3	1.6	17.0	9.4	8.3	61.9	2.5	18.7	2.6	19.4	13.4
2004	17.2	72.2	4.4	18.2	2.3	9.6	23.9	19.1	54.9	11.7	33.6	4.0	11.5	34.8	36.3	61.9	16.0	27.3	6.3	10.7	58.7
2005	6.0	55.0	2.8	25.7	2.1	19.3	10.9	37.3	51.6	23.6	32.7	11.4	15.8	72.3	43.3	52.0	26.4	31.7	13.5	16.2	83.2
2006	5.0	60.2	2.2	26.2	1.1	13.6	8.3	19.1	57.2	9.6	28.7	4.7	14.1	33.3	24.1	57.8	11.7	28.2	5.8	14.0	41.6
2007	24.5	76.7	5.6	17.4	1.9	5.9	32.0	26.1	60.6	12.2	28.4	4.7	11.0	43.0	50.6	67.5	17.8	23.7	6.6	8.8	75.0
2008	7.9	63.9	3.4	27.1	1.1	9.0	12.4	26.7	62.3	12.1	28.3	4.0	9.4	42.9	34.6	62.6	15.5	28.0	5.2	9.3	55.3
2009	28.5	74.7	4.6	12.0	5.1	13.2	38.2	64.4	72.8	17.5	19.8	6.5	7.3	88.4	92.9	73.4	22.1	17.5	11.5	9.1	126.6
2010	11.2	58.0	5.1	26.7	3.0	15.3	19.3	35.3	61.1	14.9	25.7	7.6	13.2	57.8	46.5	60.3	20.0	25.9	10.6	13.7	77.1
2011	7.0	68.5	2.3	22.5	0.9	9.0	10.3	25.3	67.4	8.0	21.3	4.2	11.3	37.5	32.3	67.6	10.3	21.5	5.2	10.9	47.8
AVG	12.2	65.5	3.4	21.2	2.1	13.3	17.7	28.8	61.1	12.4	26.6	5.4	12.3	46.6	41.0	62.8	15.8	24.7	7.5	11.5	64.3

Table 4

Vertical distribution of cysts by subregion for each survey year. For each subregion, values indicate the percentage of cysts found at a given sediment layer. Note that the 1-3 cm layer is twice the thickness of the surface (0-1) cm layer.

	Surface (0-1cm) layer			1-3 cm layer		
YEAR	WGOM	EGOM	BOF	WGOM	EGOM	BOF
1997	28.9	24.0	38.5	69.9	80.0	61.5
2004	47.4	27.1	36.5	52.6	72.9	63.5
2005	13.9	10.6	15.6	86.1	89.4	84.4
2006	20.8	18.5	19.4	79.2	81.5	80.6
2007	48.5	31.3	28.6	51.5	68.7	71.4
2008	22.9	21.7	21.6	77.1	78.3	78.4
2009	30.7	20.8	43.8	69.3	79.2	56.2
2010	24.1	25.7	27.9	75.9	74.3	72.1
2011	21.8	22.5	17.7	78.3	77.5	81.3
Average	**28.8**	**22.5**	**27.7**	**71.2**	**77.5**	**72.3**

Table 5

Statistics for cysts → blooms linear regressions. Statistically significant relationships are in bold. Where relevant, the p and R^2 values in parentheses are for regressions that include 2009 cysts and 2010 bloom (e.g. the "anomalous" bloom year for the GOM – see text in Section 3.5.)

Cysts → blooms (Relationship between cyst abundance and blooms the next year)					
Subregions	**Cyst layer**	**Subregions/Metric**	**p value***	**R^2**	**Fig. number**
WGOM+EGOM	0-1 cm	WGOM+EGOM km closed	0.0568 (0.4508)	0.48 (0.08)	8A (not shown)
WGOM+EGOM	0-3 cm	WGOM+EGOM km closed	**0.0374** (0.8688)	0.54 (0.00)	8B (not shown)
WGOM+EGOM	0-1 cm	WGOM km closed	**0.0160** (0.7077)	0.65 (0.02)	8C (not shown)
WGOM+EGOM	0-3 cm	WGOM km closed	**0.0222** (0.9764)	0.61 (0.00)	8D (not shown)
WGOM	0-1 cm	WGOM km closed	**0.0245**	0.60	Not shown
WGOM	0-3 cm	WGOM km closed	**0.0205** (0.7132)	0.62 (0.02)	Not shown
EGOM+BOF	0-1 cm	EGOM km closed	0.6731 (0.3481)	0.03 (0.13)	Not shown
WGOM+EGOM	0-1 cm	Lat. of southernmost closure	**0.0020** (0.3719)	0.82 (0.11)	10A (not shown)
WGOM+EGOM	0-3 cm	Lat. of southernmost closure	**0.0422** (0.8688)	0.52 (0.00)	10B (not shown)
WGOM	0-1 cm	Lat. of southernmost closure	**0.0023** (0.4561)	0.81 (0.08)	10C (not shown)
WGOM	0-3 cm	Lat. of southernmost closure	**0.0042** (0.9764)	0.61 (0.00)	10D (not shown)
WGOM+EGOM	0-1 cm	WGOM+EGOM cum. toxin	0.5949	0.06	Not shown
WGOM+EGOM	0-3 cm	WGOM+EGOM cum. toxin	0.5924	0.06	Not shown
WGOM+EGOM	0-1 cm	WGOM+EGOM duration	0.3888	0.15	Not shown
WGOM+EGOM	0-3 cm	WGOM+EGOM duration	0.1459	0.37	Not shown

Table 6

Statistics for blooms → cysts regressions. Statistically significant relationships are in bold.

Blooms → cysts (Relationship between bloom metrics and cysts formed later that year)					
Subregions/Metric	**Subregions**	**Cyst layer**	**p value**	**R²**	**Fig. number**
WGOM+EGOM km closed	WGOM+EGOM	0-1 cm	0.6274	0.04	Not shown
WGOM+EGOM km closed	WGOM+EGOM	0-3 cm	0.1056	0.33	Not shown
WGOM+EGOM km closed	WGOM	0-1 cm	0.6506	0.03	Not shown
WGOM+EGOM km closed	WGOM	0-3 cm	0.1787	0.24	Not shown
EGOM km closed	WGOM+EGOM	0-1 cm	0.1906	0.23	Not shown
EGOM km closed	WGOM+EGOM	0-3 cm	**0.0246**	0.54	11
Lat. of southernmost closure	WGOM+EGOM	0-1 cm	0.3237	0.14	Not shown
Lat. of southernmost closure	WGOM+EGOM	0-3 cm	0.7499	0.02	Not shown
Lat. of southernmost closure	WGOM	0-1 cm	0.3960	0.11	Not shown
Lat. of southernmost closure	WGOM	0-3 cm	0.9005	0.00	Not shown
Termination date	WGOM+EGOM	0-1 cm	**0.0277**	0.62	12A
Termination date	WGOM+EGOM	0-3 cm	**0.0112**	0.52	12B
WGOM+EGOM cum. toxin	WGOM+EGOM	0-1 cm	0.0908	0.36	Not shown
WGOM+EGOM cum. toxin/	WGOM+EGOM	0-3 cm	**0.0085**	0.62	13
WGOM+EGOM toxicity duration	WGOM+EGOM	0-1 cm	0.0588	0.39	Not shown
WGOM+EGOM toxicity duration	WGOM+EGOM	0-3 cm	**0.0084**	0.65	14